Clearance of intracellular tau protein from neuronal cells via VAMP8-induced secretion

Received for publication, March 21, 2020, and in revised form, October 3, 2020 Published, Papers in Press, October 22, 2020, DOI 10.1074/jbc.RA120.013553

Julie Pilliod[1], Alexandre Desjardins[1], Camille Pernègre[1,2], Hélène Jamann[1,2], Catherine Larochelle[1,2], Edward A. Fon[3], and Nicole Leclerc[1,2,*]

From the [1]Research Center of the University of Montreal Hospital (CRCHUM), Montréal, Canada, the [2]Département de Neurosciences, Faculté de Médecine, Université de Montréal, Montréal, Canada, and the [3]McGill Parkinson Program, Department of Neurology and Neurosurgery, Montreal Neurological Institute, McGill University, Montréal, Canada

Edited by Paul E. Fraser

In Alzheimer's disease (AD), tau, a microtubule-associated protein (MAP), becomes hyperphosphorylated, aggregates, and accumulates in the somato-dendritic compartment of neurons. In parallel to its intracellular accumulation in AD, tau is also released in the extracellular space, as revealed by its increased presence in cerebrospinal fluid (CSF). Consistent with this, recent studies, including ours, have reported that neurons secrete tau, and several therapeutic strategies aim to prevent the intracellular tau accumulation. Previously, we reported that late endosomes were implicated in tau secretion. Here, we explore the possibility of preventing intracellular tau accumulation by increasing tau secretion. Using neuronal models, we investigated whether overexpression of the vesicle-associated membrane protein 8 (VAMP8), an R-SNARE found on late endosomes, could increase tau secretion. The overexpression of VAMP8 significantly increased tau secretion, decreasing its intracellular levels in the neuroblastoma (N2a) cell line. Increased tau secretion by VAMP8 was also observed in murine hippocampal slices. The intracellular reduction of tau by VAMP8 overexpression correlated to a decrease of acetylated tubulin induced by tau overexpression in N2a cells. VAMP8 staining was preferentially found on late endosomes in N2a cells. Using total internal reflection fluorescence (TIRF) microscopy, the fusion of VAMP8-positive vesicles with the plasma membrane was correlated to the depletion of tau in the cytoplasm. Finally, overexpression of VAMP8 reduced the intracellular accumulation of tau mutants linked to frontotemporal dementia with parkinsonism and α-synuclein by increasing their secretion. Collectively, the present data indicate that VAMP8 could be used to increase tau and α-synuclein clearance to prevent their intracellular accumulation.

In AD, tau, a neuronal MAP enriched in the axon, becomes hyperphosphorylated, accumulates in the somato-dendritic compartment, and self-aggregates into insoluble filaments called paired helical filaments that form neurofibrillary tangles (1–5). Both histopathological examination of postmortem brain and PET imaging of tau pathology demonstrate a correlation to cognitive deficits in patients (6–12). The importance of tau dysfunction in neurodegeneration is further evidenced by the enrichment of tau genetic variants in patients suffering from Fronto-temporal lobar degeneration (FTLD) (5). FTLD represents 5–15% of all dementia and includes frontotemporal dementia with parkinsonism linked to chromosome 17 (FTDP-17) (5, 13–15). Over 50 mutations in the tau gene are responsible for 10–20% of FTDP-17 familial cases (15–18). Although no mutations in the tau gene have been found in AD patients, tau gene polymorphisms may be risk factors for AD and sporadic FTLD (19). A duplication of the tau gene was recently correlated to early-onset dementia with an AD clinical phenotype (20). Despite all these links, the precise role of tau in neurodegeneration remains obscure and no therapeutic strategy is available to prevent tau pathology.

In parallel to its intracellular accumulation, tau was also shown to accumulate in the extracellular space in AD. The presence of extracellular tau was revealed by its accumulation in the CSF during the progression of the disease, which was believed to correlate with neuronal cell death (21). More recently, the presence of tau in the interstitial fluid in the absence of neurodegeneration was demonstrated by microdialysis in tau transgenic mouse brain showing that tau was released by neurons *in vivo* (22). Neuronal activity was shown to increase tau release by neurons both *in vitro* and *in vivo* (23, 24). Furthermore, we reported that the induction of autophagy and/or lysosomal dysfunction increased the release of tau by primary cortical neurons (25).

Collectively, the above studies revealed that tau can be secreted by neurons. Tau secretion seems to occur in both physiological and pathological conditions. Indeed, tau is found in the CSF of control individuals but at lower levels than in AD indicating that extracellular tau could have a physiological role (26). This was noted for other cytosolic proteins such as annexin A4 and A5 that act as anticoagulant factors in the extracellular space (27). In pathological conditions, recent studies indicate that secretion of aggregated tau could be involved in cell-to-cell transmission of tau pathology in the brain (28–30). Furthermore, extracellular tau aggregates were shown to alter the protein composition of synapses and their function (31). On the other hand, secretion of aggregated proteins could act as a clearance mechanism to prevent their intracellular accumulation. This possibility was demonstrated for TDP-43 and α-synuclein (28, 32). Based on the above studies, one can conclude that the increase of tau secretion could be beneficial to neurons for three reasons: (*a*) if the secretion of neuroprotective species could be specifically increased; (*b*) if the

This article contains supporting information.

* For correspondence: Nicole Leclerc, Nicole.leclerc@umontreal.ca.

secretion of intracellular toxic tau species could be increased to prevent their accumulation; and (*c*) if the increase of tau secretion would become a means to make more accessible to a therapeutic agent intracellular tau species involved in tau-mediated neurodegeneration. Indeed, extracellular tau is presently a therapeutic target in several clinical trials where an anti-tau antibody is used to sequester its toxic species (33). The increase of tau secretion combined with the capture of extracellular toxic tau species by an antibody could be an efficient approach to prevent the intracellular accumulation of these species and their propagation in the brain.

The secretory pathway of pathological tau is still largely unknown, limiting the capacity of modulating it and unequivocally demonstrate its contribution to tau clearance. The secretion of tau occurs through unconventional secretory pathways, which involve structures such as late endosomes, autophagosomes, and lysosomes, membranous organelles that can fuse with the plasma membrane to release their content (31). We recently reported that Rab7A associated with late endosomes participates in tau secretion (34). In the present study, we examined whether tau secretion could be increased by overexpression of VAMP8, an R-SNARE associated with late endosomes (35–37). Our results demonstrate that overexpression of VAMP8 increased WT and mutated human tau secretion resulting in a decrease of their intracellular accumulation. The increase of acetylated tubulin resulting from tau overexpression was significantly reduced upon tau secretion by VAMP8. VAMP8-positive vesicles preferentially associated with late endosomes could fuse with the plasma membrane as revealed by TIRF microscopy. Tau secreted upon VAMP8 overexpression was dephosphorylated and cleaved at the C-terminal. Last, VAMP8 overexpression could also reduce the intracellular levels and increased the extracellular levels of α-synuclein. Altogether, the above observations indicate that VAMP8 could be used to prevent the intracellular accumulation of proteins linked to neurodegenerative diseases.

Results

Increase of tau secretion and decrease of intracellular tau upon overexpression of VAMP8

In a previous study, we reported that late endosomes participated in tau secretion in both nonneuronal and neuronal cells (34). The R-SNARE VAMP8 is found on late endosomes and is involved in exocytosis (35–41). We therefore examined whether overexpression of VAMP8 could increase tau secretion. Overexpression of VAMP8 and tau in the N2a cells resulted in a reduction of tau in the cell lysate and an increase of tau in the culture medium compared with tau overexpression alone (Fig. 1*A*). Quantification of tau signal revealed that tau protein levels were significantly decreased in the cell lysate and significantly increased in the culture medium (Fig. 1, *B* and *C*). Similar results were obtained when the amount of tau in the cell lysate and medium was measured using the MSD MULTI-SPOT phospho(Thr-231)/total tau kit (Fig. 1, *D* and *E*). In some experiments, intracellular tau protein levels in cells overexpressing VAMP8 were as low as half of those of tau overexpression alone. The amount of lactate dehydrogenase (LDH), a biomarker of cellular cytotoxicity and cytolysis, was measured in the medium to make sure that the overexpression of VAMP8 did not alter the neuronal plasma membrane integrity and neuronal survival (Fig. 1*F*). The low protein levels of endogenous VAMP8 in N2a cells prevented us from examining its contribution to the basal tau secretion upon tau overexpression. As illustrated in Fig. S1, the detection of VAMP8 in N2a cells by Western blotting was only possible when it was overexpressed. We then examined whether VAMP8 would exert the same effect on overexpressed tau in hippocampal slices prepared from P4–P5 mice. After 48 h in culture, hippocampal slices were transduced either with a lentivirus encoding GFP, a bicistronic lentivirus encoding VAMP8 and GFP, a bicistronic lentivirus encoding tau and DsRed, and the lentivirus encoding GFP or with the bicistronic lentivirus encoding tau and the one encoding VAMP8. The expression of tau in the slices was confirmed by the detection of DsRed (Fig. S2). The amount of tau in the culture medium was measured using the MSD MULTI-SPOT mouse total tau assay as described (34, 42). The amount of tau released in the medium in control before conditions and VAMP8 overexpression alone was similar indicating that VAMP8 did not increase the secretion of endogenous tau (Fig. 1*G*). As noted in N2a cells, the secretion of overexpressed tau was increased upon VAMP8 overexpression in hippocampal slices compared with tau overexpression alone (Fig. 1, *G* and *H*). The amount of LDH was measured in the medium of hippocampal slices to confirm that the lentivirus infection did not alter the neuronal plasma membrane integrity and neuronal survival (Fig. 1*I*).

Collectively, the above results indicated that VAMP8 enhanced tau secretion resulting in its decrease in the cell lysate. To confirm that it was the case, we verified whether the decrease of tau in the cell lysate was not caused by a decrease of its expression. Tau expression was measured by quantitative PCR revealing that it was not significantly decreased upon overexpression of VAMP8 (Fig. S3). A decrease of intracellular tau could also result from an increase of its degradation. To test this, N2a cells overexpressing either tau alone or tau and VAMP8 were treated either with bafilomycin or chloroquine to block autophagy, a degradative pathway known to contribute to tau degradation (43). Upon these treatments, no increase of tau in the cell lysate was noted indicating that the decrease of tau in the cell lysate was not caused by an increase of its degradation when VAMP8 was overexpressed (Fig. 2, *A–D*). The increase of LC3II in the cell lysate was noted when cells were treated either with chloroquine or bafilomycin indicating that these drugs were effective in blocking autophagy (Fig. 2, *E* and *F*). Tau can also be degraded by the proteasome (43). An inhibition of the proteasome activity by MG132 treatment was tested to verify if it increased the amount of tau in the lysate in cells overexpressing tau and VAMP8. No increase of tau was noted in the cell lysate in MG132-treated cells (Fig. 2, *G* and *H*). The efficacy of MG132 in blocking the proteasome was confirmed by the increase of the amount of ubiquitinated proteins in the cell lysate (Fig. 2*I*). Collectively, the above results confirmed that the intracellular decrease of tau resulted from an increase of its secretion rather than by an increase of its degradation upon VAMP8 overexpression.

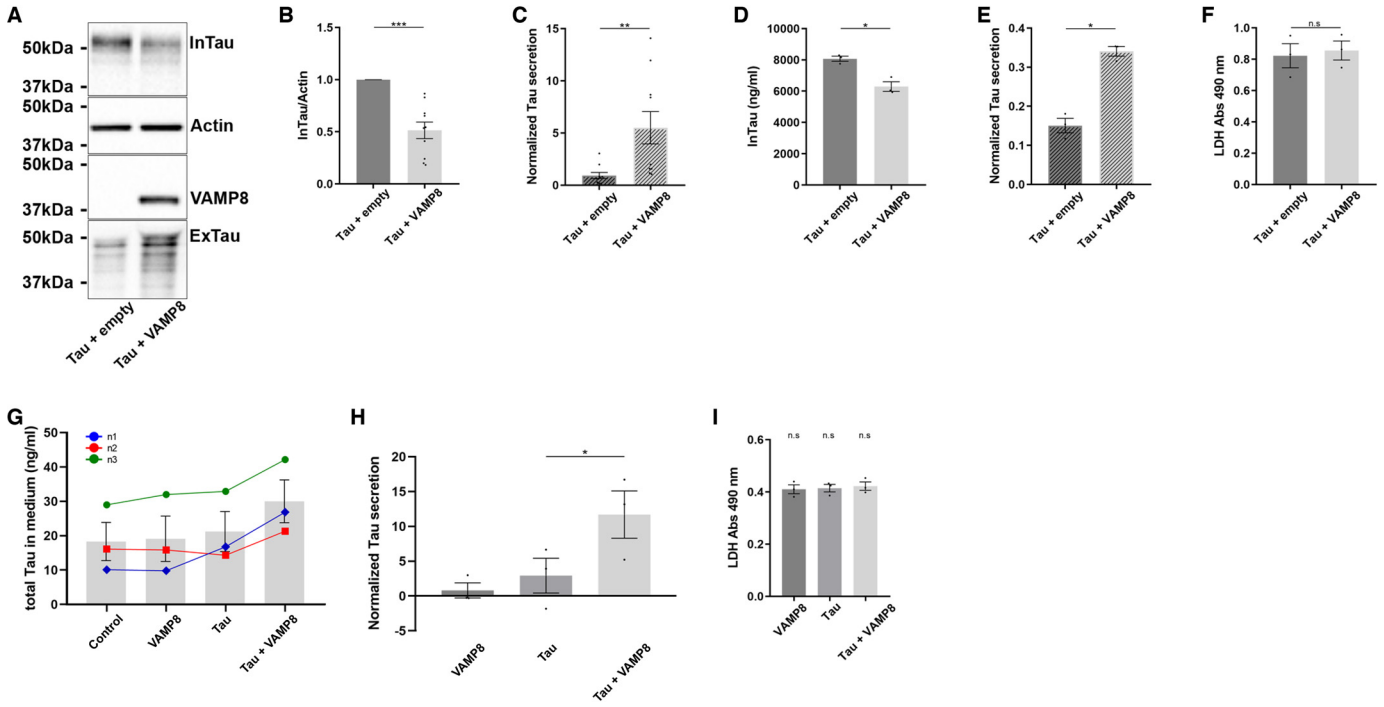

Figure 1. Overexpression of VAMP8 results in a decrease of intracellular tau and an increase of extracellular tau. N2a cells were transfected either with Flag-4R-TAU and EGFP-empty plasmids or Flag-4R-TAU and GFP-VAMP8 plasmids for 48 h. *A,* representative Western blotting with the antibody A0024 of the cell lysate and the medium revealing that the overexpression of VAMP8 decreased intracellular tau (*InTau*) and increased extracellular tau (*ExTau*). *B,* densitometry analysis of the A0024 signal of InTau. Actin was used as a loading reference. *C,* densitometry analysis of the A0024 signal of ExTau. Normalized tau secretion corresponds to the ratio ExTau/InTau. InTau was normalized with the actin signal; $n = 10$. *D*, the amount of InTau (ng/ml) was measured using MSD MULTI-SPOT. *E*, the amount of ExTau was measured using MSD MULTI-SPOT and normalized with InTau. *F,* quantification of the levels of LDH in the medium of N2a cells; $n = 3$. *G,* hippocampal slices were prepared from P4-P5 mice. After 5 days in culture, hippocampal slices were transduced either with a lentivirus encoding GFP (*control*), a bicistronic lentivirus encoding VAMP8 and GFP (*VAMP8*), a bicistronic lentivirus encoding Tau and DsRed (*Tau*), or with the lentivirus encoding Tau and the one encoding VAMP8 (*Tau + VAMP8*). The amount of tau in the culture medium (ng/ml) was measured using MSD MULTI-SPOT mouse total Tau assay. *H,* quantification of tau in the medium of hippocampal slices. The amount of ExTau in the medium of slices overexpressing VAMP8, Tau, or VAMP8 and Tau was normalized to that of ExTau in control medium (*GFP*); $n = 3$. *I,* quantification of the levels of LDH in the medium of hippocampal slices; $n = 3$. Data represent scatter plot and mean ± S.E. Each *dot* corresponds to a *n.* *, $p < 0.05$; **, $p < 0.01$; and ***, $p < 0.001$.

Tau secretion by VAMP8 reduces the increase of acetylated tubulin upon its overexpression

We examined whether the increase of tau secretion and its decrease in the cell lysate by the overexpression of VAMP8 were sufficient to reverse alterations induced by the overexpression of tau. In N2a cells, tau overexpression was accompanied by an increase of acetylated tubulin indicating that microtubules were more stable upon tau binding as previously reported by others (Fig. 3*A*) (44, 45). This increase of acetylated tubulin was significantly reduced when tau secretion was induced by the overexpression of VAMP8 (Fig. 3*B*). From the above observations, one can conclude that the increase of tau secretion by VAMP8 is sufficient to reverse alterations induced by tau accumulation.

Visualization of the fusion of VAMP8-positive vesicles with the plasma membrane by TIRF microscopy

GFP-tau and RFP-VAMP8 were co-expressed in N2a cells to examine their co-localization. Thirty minutes before fixing the cells, the medium containing tau was removed and replaced by fresh medium as a means to stimulate tau secretion that reaches a plateau over 24-48 h (46). VAMP8 was found in vesicles that were located at the cell center and at the periphery close to the plasma membrane (Fig. 4*A*). Surprisingly, for several VAMP8-positive vesicles, a black area corresponding to the size of the vesicle was found in tau labeling revealing that no tau was present in this area (Fig. 4*A*). We then explored whether this depletion of tau in the cytoplasm was correlated to its secretion by VAMP8-positive vesicles. Tau secretion by VAMP8-positive vesicles would involve their fusion with the plasma membrane. To demonstrate this, (TIRF) microscopy on live cells allowing the detection of vesicle fusion with the plasma membrane was employed. Indeed, this microscopy allows the visualization of a fluorescent signal at the contact area between a cell and a glass coverslip where the fusion of vesicle with the plasma membrane can be detected. A sudden reduction of the fluorescence indicates that a fusion event had happened. This reduction has to occur in 500 ms for corresponding to a fusion event (40). Using TIRF microscopy, VAMP8-positive vesicles were found at the contact area between the plasma membrane of the cell and the coverslips where the fusion event can be observed (Fig. 4*B*). A sudden reduction of VAMP8 signal occurred in 500 ms indicating that the VAMP8-positive vesicle had fused with the plasma membrane. The sudden reduction of fluorescence is caused by the dispersion of the fluorescent signal upon the event fusion. After this event of fusion, a decrease of tau labeling was noted in the area where the VAMP8 signal disappeared indicating that tau was secreted (Fig. 4*C*). For some VAMP8-positive vesicles, the

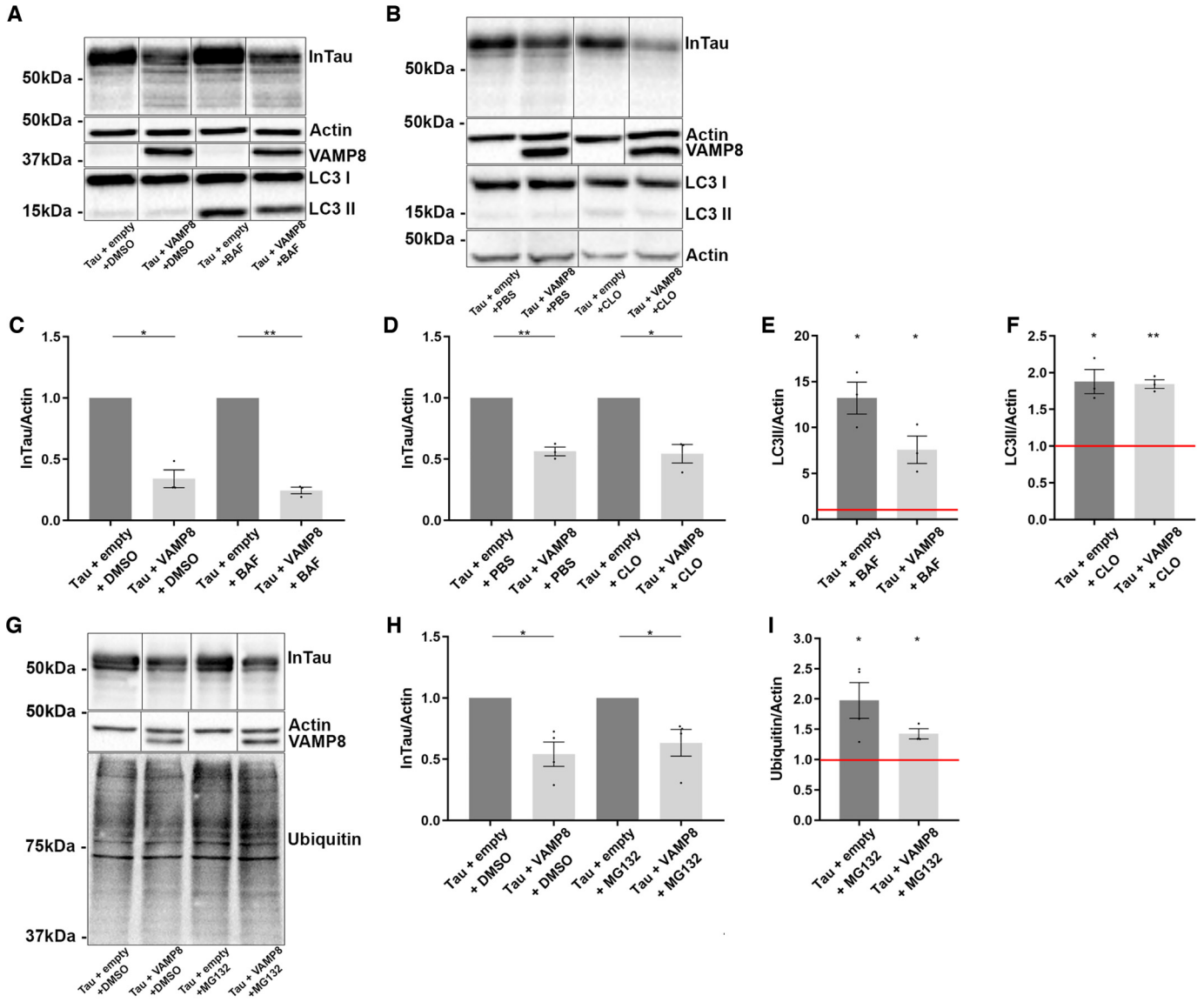

Figure 2. The decrease of intracellular tau upon VAMP8 overexpression is not caused by its degradation but rather by its secretion. N2a cells overexpressing either Flag-4R-TAU and EGFP-empty plasmids or Flag-4R-TAU and GFP-VAMP8 plasmids were treated either with bafilomycin (*BAF*) or chloroquine (*CLO*) to block autophagy and MG132 to inhibit the proteasome. *A* and *B*, Western blotting analysis with the antibody A0024 of the cell lysate revealed that no increase of InTau was noted when the cells were treated either with BAF or CLO. *C* and *D*, densitometry analysis of the A0024 signal of InTau in cells treated either with BAF (DMSO as control) or CLO (PBS as control). *E* and *F*, densitometry analysis of the LC3II signal in cells treated either with BAF or CLO. The efficacy of BAF and CLO was demonstrated by an increase of LC3II in the cell lysate compared with control conditions (*red bar*). *G*, Western blotting analysis with the antibody A0024 of the cell lysate revealed that no increase of InTau was noted when the cells were treated with MG132. *H*, densitometry analysis of A0024 signal of InTau in cells treated either with MG132 or DMSO (*control*). *I*, densitometry analysis of ubiquitin signal in cells treated either with MG132 or DMSO. The efficacy of MG132 was shown by an increase of ubiquitin staining compared with the control condition (*red bar*). *Black frames* were used to mark the splice sites of immunoblot images. Data represent scatter plot and mean ± S.E., minimum $n = 3$. Each *dot* corresponds to a *n*. *, $p < 0.05$; **, $p < 0.01$.

reduction of fluorescence occurred over a period longer than 500 ms, indicating that these vesicles moved out of the field without any fusion event with the plasma membrane (Fig. S4*A*). When a vesicle moved out of the field without any fusion with the plasma membrane, no decrease of tau labeling was observed in the area where the vesicle was observed (Fig. S4*A*). The labeling of tau in the vicinity of the plasma membrane was visualized by TIRF. Two pools of tau, one pool attached to microtubules and one free pool found in the cytoplasm, were observed as expected when tau is overexpressed (Fig. S4*B*). From the above observations, one could conclude that tau was secreted by the fusion of VAMP8-vesicles with the plasma membrane.

VAMP8-positive vesicles preferentially co-localize with Rabs found on late endosomes

N2a cells were co-transfected with VAMP8, tau, and a Rab GTPase, markers of different endosomal compartments, to determine in which endocytotic compartment VAMP8 was localized (47). Very limited co-localization was observed with Rab5, a marker of the early endosomes (data not shown), and with Rab11, a marker of the recycling endosomes where VAMP8 was reported in a previous study (Fig. 5, *A* and *B*) (40, 47). A partial co-localization of VAMP8 was noted with Rab7A, a marker of late endosomes (Fig. 5, *A* and *B*) (48). The most significant co-localization was observed with Rab9, a Rab that

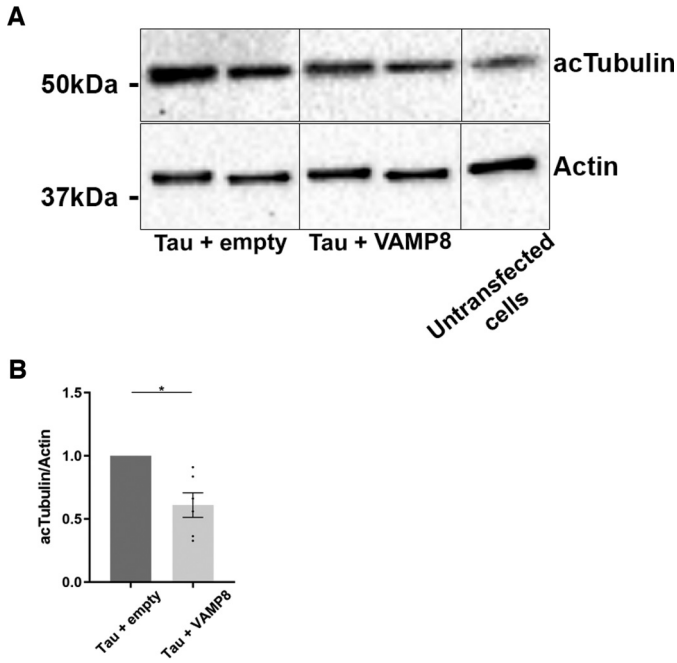

Figure 3. The decrease of intracellular tau by VAMP8 overexpression reduces the increase of acetylated tubulin upon tau overexpression. N2a cells were transfected either with Flag-4R-TAU and EGFP-empty plasmids or Flag-4R-TAU and GFP-VAMP8 plasmids for 48 h. *A,* Western blotting analysis with the antibody directed against acetylated tubulin (*acTubulin*) of the cell lysate revealed that the overexpression of VAMP8 decreased the amount of acTubulin. *B,* densitometry analysis of acTubulin signal. *Black frames* were used to mark the splice sites of immunoblot images. Data represent scatter plot and mean ± S.E. $n = 6$. Each *dot* corresponds to a *n*. *, $p < 0.05$.

enters the endosomal pathway at the Rab5-to-Rab7A transition (Fig. 5, *A* and *B*) (49). Interestingly, Rab7A- and Rab9-positive vesicles often presented a doughnut shape where VAMP8 staining was concentrated at the center of the doughnut (Fig. 5*A*).

Characterization of tau phosphorylation upon VAMP8 overexpression

We and others reported that secreted tau presented low levels of phosphorylation and was cleaved at the C-terminal (34, 42, 50–52). These modifications were examined for intracellular and extracellular tau upon the overexpression of VAMP8 using the antibody Tau-46 nonreactive to tau cleaved at the C-terminal, the antibody Tau-1 recognizing dephosphorylated tau at the epitope 195-202, an antibody recognizing tau phosphorylated at Ser-199/Ser-202 and the antibody AT180 directed against tau phosphorylated at Thr-231/Ser-235. Mesoscale was used to detect tau phosphorylation at Thr-231 (53, 54). Total tau in the cell lysate and medium was revealed using the antibody A0024 (Fig. 6*A*). Tau found in the cell lysate was reactive to the antibody Tau-46, whereas tau in the medium could not be detected by this antibody revealing that tau secreted upon the overexpression of VAMP8 was cleaved at the C-terminal as noted for tau overexpression alone (Fig. 6*B*). In N2a cells overexpressing VAMP8, intracellular tau was not dephosphorylated more at the epitope recognized by the Tau-1 antibody than in cells overexpressing tau alone as revealed by no change of the Tau-1/total tau ratio (Fig. 6, *C* and *D*). This was consistent with no change of tau phosphorylation at Ser-199/Ser-202, two sites comprised in the epitope of the Tau-1 antibody (Fig. 6, *E* and *F*). However, intracellular tau was significantly less phosphorylated at Thr-231/Ser-235 as revealed by the AT180/total tau ratio (Fig. 6, *E* and *G*). The phosphorylation levels of extracellular tau were also affected by VAMP8 overexpression. Upon the overexpression of VAMP8, extracellular tau secreted presented a higher Tau-1/total tau ratio than tau overexpression alone (Fig. 6, *H* and *I*). This indicated that secreted tau was more dephosphorylated upon VAMP8 overexpression. Consistent with this, a decrease of the antibody AT180 signal was noted in the medium (Fig. 6, *J* and *K*). No signal was detected with the antibody directed against tau phosphorylated at Ser-199/Ser-202 in the medium. The MSD MULTI-SPOT phospho(Thr-231)/total tau kit was used to examine intracellular and extracellular Thr-231 phosphorylation (Fig. 6, *L* and *M*). The phosphorylation of Thr-231 was decreased in the cell lysate but was not altered in the medium when VAMP8 was overexpressed. The fact that the phosphorylation at Thr-231/Ser-235 was decreased in the cell lysate of cells co-overexpressing tau and VAMP8 prompted us to examine whether phosphorylation was a determinant factor in tau secretion upon VAMP8 overexpression. To test this, a mutant either mimicking phosphorylation of tau or not phosphorylable at 12 sites known to be phosphorylated in AD including Thr-231 and Ser-235 were overexpressed with VAMP8 in N2a cells (Fig. 6, *N–P*). Both mutants were more secreted when VAMP8 was overexpressed as noted for WT tau indicating that phosphorylation at these sites did not regulate tau secretion by VAMP8 (Fig. 6*P*). Last, we examined whether tau secreted upon VAMP8 overexpression was more oligomeric and presented more conformational changes than tau secreted by tau overexpression alone (Fig. S5). No changes were observed with the antibody T22 recognizing oligomeric tau and the antibody MC1 directed against tau presenting conformational changes (55, 56). Collectively, the above results revealed that secreted tau upon the overexpression of VAMP8 presented modifications similar to those of tau secreted upon tau overexpression alone.

Secretion of tau mutants linked to FTDP and α-synuclein is increased by VAMP8

We examined whether VAMP8 was efficient in secreting tau mutants linked to FTDP as it was for WT tau (57). The co-overexpression of VAMP8 either with tau mutant P301L or R406W resulted in their decrease in the cell lysate and their increase in the culture medium, although VAMP8 protein levels were lower in tau mutants expressing cells than in WT tau expressing cells (Fig. 7, *A–C*).

We also tested whether VAMP8 could induce the secretion of other proteins involved in neurodegenerative diseases and known to be secreted by neurons. The overexpression of VAMP8 on the secretion of α-synuclein, a protein involved in Parkinson's disease, was tested (58, 59). As noted for tau, the intracellular protein levels of α-synuclein were decreased upon the overexpression of VAMP8 (Fig. 7, *D* and *E*). This

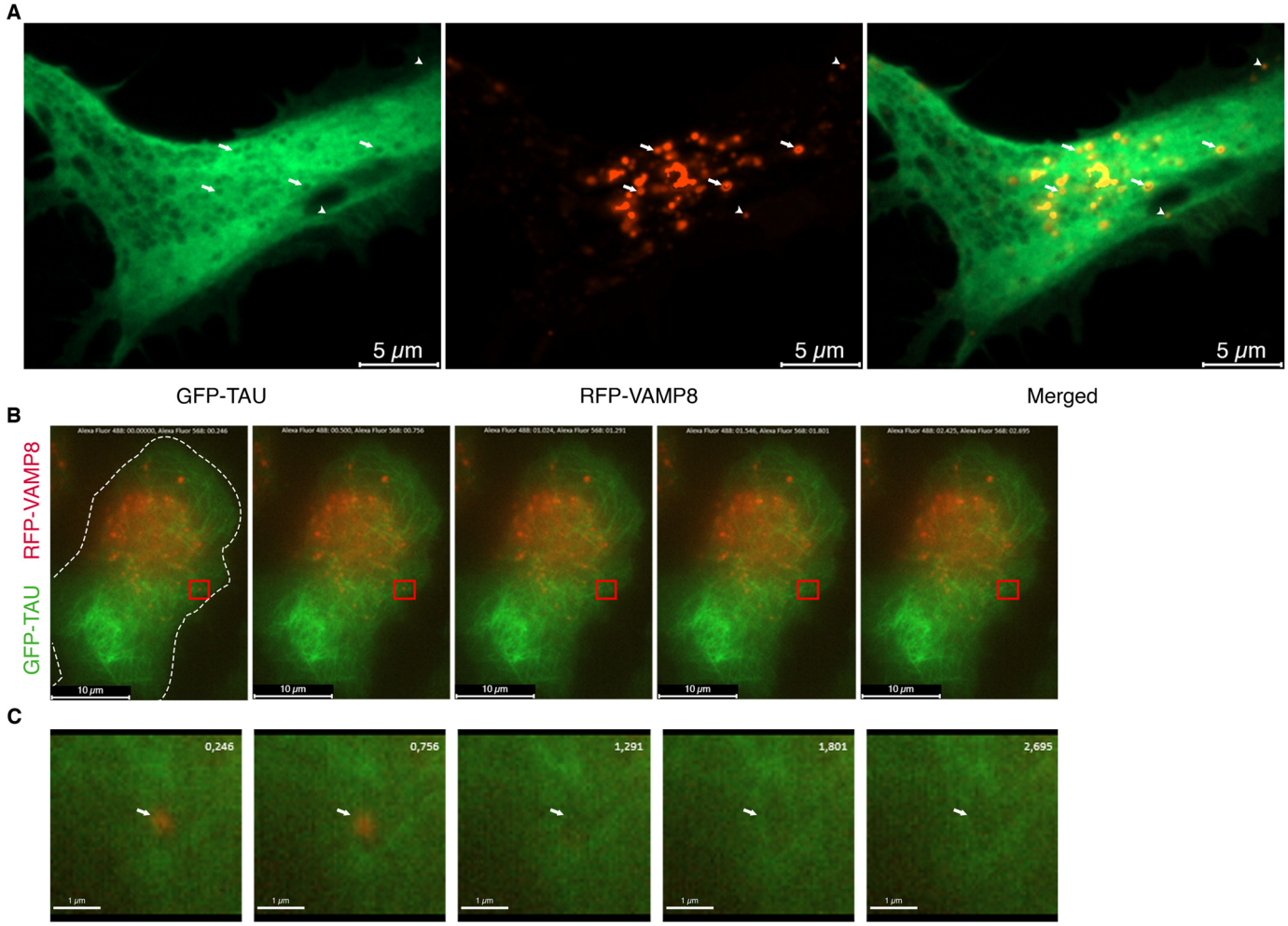

Figure 4. VAMP8-positive vesicles fuse with the plasma membrane as visualized by TIRF microscopy. N2a cells were transfected with GFP-4R-TAU and RFP-VAMP8 plasmids for 24 h. Secretion of tau was stimulated by replacing the medium containing tau with fresh medium for 30 min either before fixation of the cells or TIRF microscopy on live cells. *A*, representative image of a cell overexpressing GFP-4R-TAU and RFP-VAMP8. VAMP8-positive vesicles (*red*) were found at the cell center (*white arrows*) and in the periphery close to the plasma membrane (*white arrowheads*). VAMP8-positive vesicles often co-localized with *black areas* of the size of the vesicles in tau staining indicating that tau has been released (*white arrows* in tau image); $n = 3$. *B*, representative live-cell TIRF images of a cell transfected with GFP-4R-TAU and RFP-VAMP8 plasmids. *Dashed lines* indicate the boundary of the cell body. The images were taken in the TIRF plane to demonstrate that several VAMP8-positive vesicles were found at the contact area between the plasma membrane of the cell and the coverslips where fusion event can be observed. *C*, the *inset* (*red square*) in *B* was enlarged. RFP-VAMP8-positive vesicle, indicated by the *white arrow*, disappeared in 500 ms (756 ms to 1.291 s) in the TIRF plane. A decrease of tau staining (1,291 ms to 2,695 ms) was noted in the area where the VAMP8-positive vesicle disappeared (*white arrow*). $n = 6$.

intracellular decrease was accompanied by an increase of extracellular α-synuclein (Fig. 7*F*). The above observations indicate that VAMP8 could be used for clearance of pathological proteins involved in neurodegenerative diseases.

Discussion

In the present study, we reported that the overexpression of VAMP8 increased tau secretion resulting in its intracellular decrease both in N2a cells and hippocampal slices. Upon this intracellular decrease of tau, the increase of acetylated tubulin, caused by the stabilizing effects of overexpressed tau on microtubules, was reduced. VAMP8 was preferentially associated with late endosomes as revealed by its co-localization either with Rab7A- or Rab9-positive structures. Using TIRF microscopy, it was possible to observe the fusion of VAMP8-positive vesicles with the plasma membrane, which resulted in depletion of the tau signal in the cytoplasm. Both intracellular and extracellular tau were less phosphorylated when VAMP8 and tau were overexpressed than upon tau overexpression alone. VAMP8 also increased the secretion of the tau mutants, P301L and R406W, and α-synuclein. Collectively the above observations indicate that the overexpression of VAMP8 could be used to increase the secretion of proteins involved in neurodegenerative diseases and prevent their intracellular accumulation and toxicity.

VAMP8 was previously found on late and recycling endosomes depending on the cell types (35–37, 40, 60). In N2a cells used in the present study, VAMP8 was preferentially found on late endosomes that we reported to be involved in tau secretion (34). Several studies demonstrated the contribution of VAMP8 in exocytosis (38–41). Consistent with such a role, it was demonstrated that VAMP8 found on recycling endosomes was involved in their fusion with the plasma membrane (40). Our results indicate that VAMP8 could also participate in the fusion

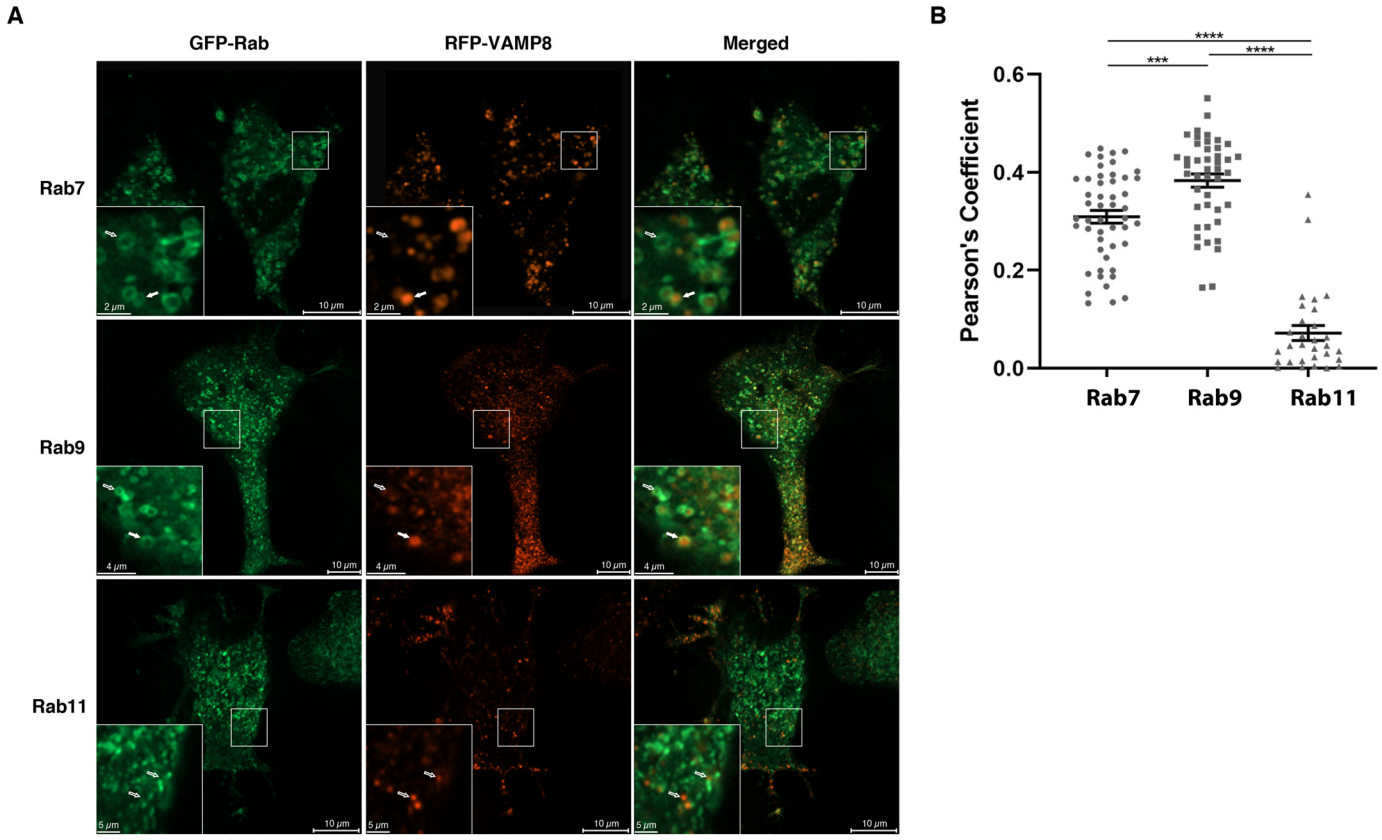

Figure 5. VAMP8-positive vesicles preferentially co-localize with Rab GTPases associated with late endosomes. N2a cells were transfected with a GFP-Rab (Rab7, Rab9, or Rab11), RFP-VAMP8 and Flag-4R-TAU plasmids for 48 h to determine in which endocytic compartment VAMP8 was localized. For each set of images, the Rab is *green* and VAMP8 in *red*. *Full white arrows* were used to indicate co-localization between VAMP8 and a Rab, whereas *empty white arrows* were used to indicate the lack of co-localization between VAMP8 and a Rab. *A,* very limited co-localization was observed with Rab11, a marker of the recycling endosomes, whereas a partial co-localization was noted with Rab7 and Rab9, two markers of the late endosomes. Interestingly, VAMP8 staining was often found at the center of the Rab7- and Rab9-positive vesicles. *B,* Pearson's coefficients for VAMP8 and Rabs. The most significant co-localization was observed with Rab9. The co-localization of VAMP8 with Rabs was quantified with Imaris software. Data represent a scatter plot and mean ± S.E. $n = 49$ cells for Rab7, $n = 44$ cells for Rab9, and $n = 30$ cells for Rab11. ***, $p < 0.001$; ****, $p < 0.0001$.

of late endosomes with the plasma membrane in neuronal cells. In these cells, VAMP8-positive vesicles contained tau that could be released upon their fusion with the plasma membrane. VAMP8 presents a very low expression in the brain and therefore the role of endogenous VAMP8 in tau secretion by neurons is debatable (41). However, such a possibility cannot be completely ruled out because it could explain why a very low amount of tau is released in both normal and pathological conditions (see below). Another possibility would be that a SNARE playing a role similar to that of VAMP8 in neurons could be involved in tau secretion by promoting the fusion of late endosomes with the plasma membrane. Such a SNARE remains to be identified. In a recent study, VAMP8 was shown to contribute to an unconventional secretion pathway involving the endoplasmic reticulum and late endosomes (61). In contrast to our results, no intracellular decrease of the secreted protein was reported upon VAMP8 overexpression. This indicates that VAMP8 could contribute to secretion by several pathways presenting different efficacy at reducing the intracellular levels of the secreted proteins. In this recent study, the role of VAMP8 in tau and α-synuclein secretion was not examined.

In the present study, VAMP8 was found on both Rab7A- and Rab9-positive structures supporting a role of the endolysosomal system in tau secretion upon VAMP8 overexpression. This is consistent with our previous study demonstrating that Rab7A was involved in tau secretion (34). Interestingly, at early stages of AD when tau intracellular accumulation occurs, Rab7A is up-regulated and there is an accumulation of endosomal structures (62–66). Based on our previous and present data, one can conclude that these changes could result in an increase tau secretion, which could explain its increase in the CSF (67, 68). In our previous study reporting that Rab7A was involved in tau secretion, suppression of Rab7A resulted in both a decrease of intracellular tau and tau secretion. In the present study, we showed that VAMP8 overexpression resulted in a decrease of intracellular tau but an increase of tau secretion. This apparent discrepancy could be explained by the fact that Rab7A has two roles: 1) it is involved in tau secretion because of its localization in the endolysosomal system and 2) it is involved in tau degradation pathway by the proteasome as discussed in our previous study (34). Indeed, Rab7A was shown to be involved in the degradation of proteins by the proteasome (69). The roles of Rab7A in secretion and degradation might vary from one cell type to another. In N2a cells, upon the overexpression of VAMP8 forcing the endolysosomal secretory pathway, Rab7A might be more involved in tau secretion than

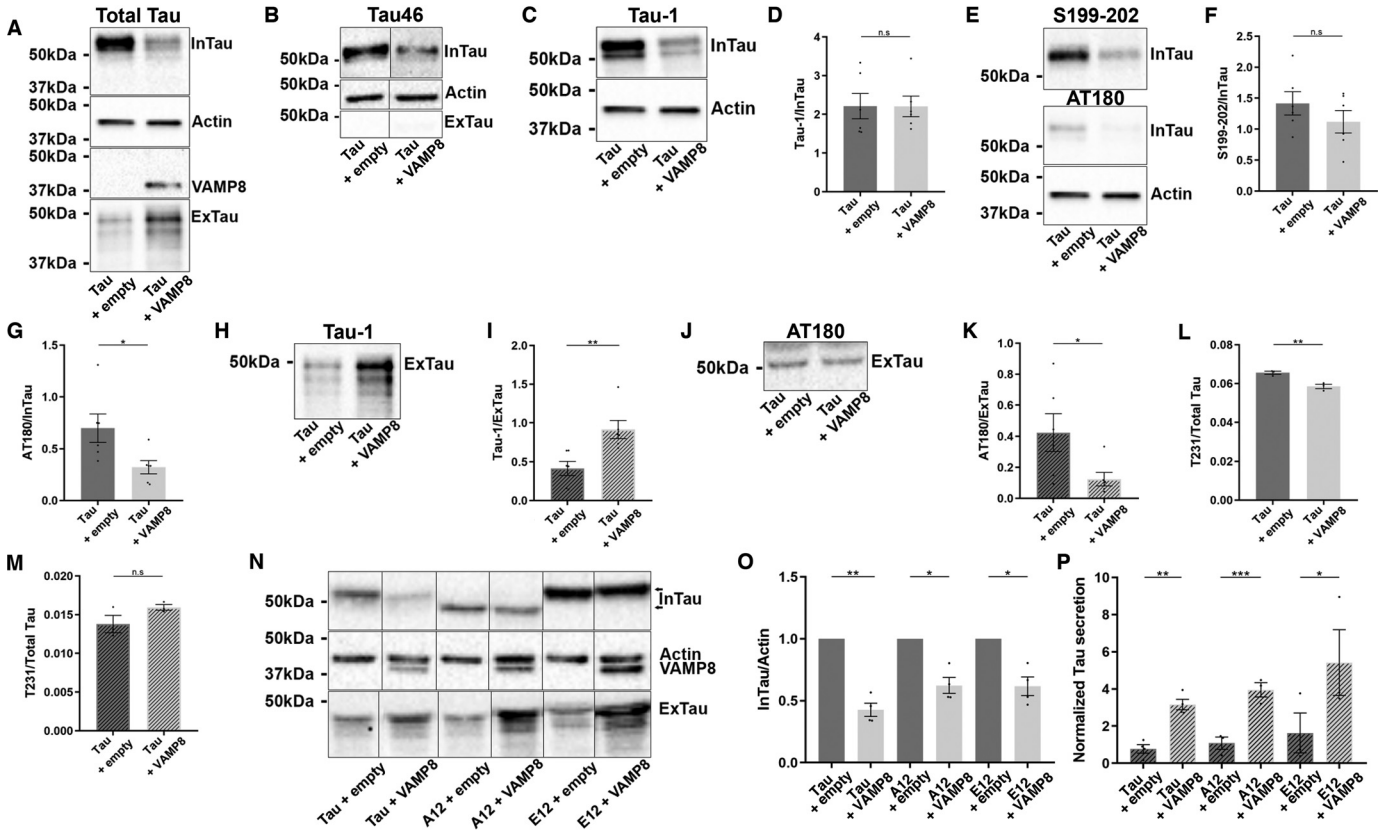

Figure 6. The overexpression of VAMP8 decreases the phosphorylation of intracellular and extracellular tau. N2a cells were transfected either with Flag-4R-TAU and EGFP-empty plasmids or Flag-4R-TAU and GFP-VAMP8 plasmids for 48 h. *A,* Western blotting analysis with the A0024 antibody of the cell lysate and medium. *B,* Western blotting analysis with the antibody Tau-46 of the cell lysate and medium. *C,* Western blotting analysis with the Tau-1 antibody of the cell lysate. *D,* densitometry analysis of Tau-1 signal of InTau; $n = 6$. *E,* Western blotting analysis with the antibody recognizing tau-phosphorylated Ser-199/Ser-202 and the antibody AT180 of the cell lysate. *F,* densitometry analysis of Ser-199/Ser-202 antibody signal of InTau; $n = 6$. *G,* densitometry analysis of AT180 signal of InTau; $n = 6$. *H,* Western blotting analysis with the antibody Tau-1 of ExTau. *I,* densitometry analysis of Tau-1 signal of ExTau; $n = 6$. *J,* Western blotting analysis with the antibody AT180 of ExTau; $n = 6$. *K,* densitometry analysis of AT180 signal of ExTau; $n = 6$. *L,* phosphorylation levels of Thr-231 of InTau measured by mesoscale. *M,* phosphorylation levels of Thr-231 of ExTau measured by mesoscale; $n = 6$. *N,* Western blotting analysis with the A0024 antibody of the cell lysate and medium of N2a cells either overexpressing a tau mutant mimicking phosphorylation (E12) or a nonphosphorylable tau mutant (A12) at 12 sites known to be phosphorylated in AD with VAMP8. *O,* densitometry analysis of the A0024 signal of InTau from A12 and E12 tau mutants. *P,* densitometry analysis of the A0024 signal of ExTau from A12 and E12 tau mutants; $n = 4$. The same actin Western blotting was used in *A*, *C,* and *E*. *Black frames* were used to mark the splice sites of immunoblot images. Data represent mean ± S.E. Each *dot* corresponds to a *n*. *, $p < 0.05$; **, $p < 0.01$; ***, $p < 0.001$.

tau degradation. Furthermore, VAMP8 co-localization was stronger with Rab9 than Rab7A indicating that the VAMP8 secretory pathway might be different from the pathway activated by Rab7A alone. Last, it is important to mention that the endolysosomal pathway might differ from one cell type to another generating apparent discrepancies. As mentioned above, in the present study, VAMP8 was found on structures containing Rab9 indicating that this Rab could contribute to tau secretion (47). Rab9-positive endosomes were reported to be involved in unconventional secretion (61). This pathway was named misfolding-associated protein secretion (MAPS). This secretory pathway is initiated by an endoplasmic reticulum-associated deubiquitinase, USP19 that has a unique chaperone activity. UPS19 uses its chaperone activity to recruit at the surface of the endoplasmic reticulum-misfolded proteins, which subsequently enter late endosomes containing Rab9. Tau, α-synuclein, TDP-43, and SOD1 were shown to be secreted by this pathway (70).

In recent years, the endolysosomal system was reported to be involved in tau degradation through Rab35 and the endosomal sorting complexes required for transport (ESCRT) (71). Our present results demonstrate the contribution of this system to tau secretion. From the above observations, one can speculate that when tau enters the endolysosomal system, it has access to at least two pathways, one involved in its degradation and one involved in its secretion. In pathological conditions where this system has been shown to be altered, the secretion pathway might become more active resulting in an increase of tau in the CSF. However, it would not be sufficient to prevent tau intracellular accumulation. Interestingly, genetic variation of genes involved in the endolysosomal system was associated with late-onset AD (72).

Upon VAMP8 overexpression, a decrease of intracellular tau phosphorylation was noted at the epitope Thr-231/Ser-235 using the antibody AT180 and a decrease at Thr-231 using mesoscale. No change of phosphorylation was detected with an antibody directed against phosphorylated Ser-199/Ser-202. These results indicate that VAMP8 overexpression could contribute to reduce both tau accumulation and phosphorylation at certain sites. In the medium, an increase of the Tau-1

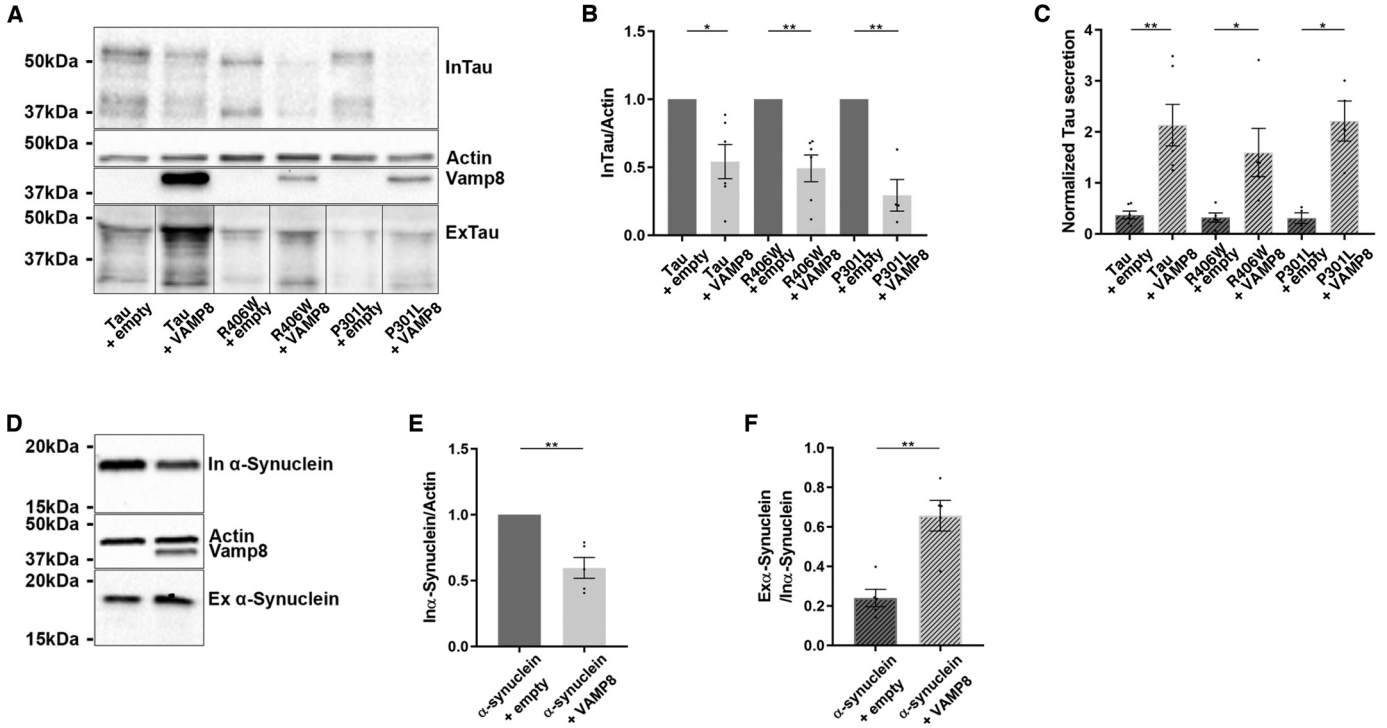

Figure 7. VAMP8 increases the secretion of tau mutants linked to FTDP and α-synuclein. N2a cells were transfected either with a tau mutant (P301L or R406W) and EGFP-empty plasmids or tau mutant (P301L or R406W) and GFP-VAMP8 plasmids for 48 h. *A,* Western blotting analysis with the A0024 antibody of the cell lysate and medium. *B,* densitometry analysis of A0024 signal of InTau. *C,* densitometry analysis of A0024 signal of ExTau; $n = 4$. *D,* Western blotting analysis with the anti-α-synuclein antibody of the cell lysate and medium of the cells overexpressing VAMP8 and α-synuclein. As noted for tau, VAMP8 decreased intracellular α-synuclein and increased extracellular α-synuclein. *E,* densitometry analysis of the anti-myc or α-synuclein antibody signal in the cell lysate. *F,* densitometry analysis of the anti-myc or α-synuclein antibody signal in the medium; $n = 3$. *Black frames* were used to mark the splice sites of immunoblot images. Data represent scatter plot and mean ± S.E. Each *dot* corresponds to a *n*. *, $p < 0.05$; **, $p < 0.01$.

antibody staining was noted upon VAMP8 overexpression indicating that tau was more dephosphorylated at this epitope than upon tau overexpression alone. Furthermore, a decrease of tau phosphorylation was found at the epitope Thr-231/Ser-235 as noted for intracellular tau. We previously reported that tau secretion by HeLa cells was increased upon its hyperphosphorylation (50). In the present study, phosphorylation of tau did not seem to modulate tau secretion by N2a cells upon the overexpression of tau alone or the overexpression of tau with VAMP8 as revealed by using tau mutants either mimicking hyperphosphorylation or not phosphorylable. However, there was a tendency for E12 to be more secreted by N2a cells than A12 and WT tau after normalization with intracellular tau. When mutants mimicking phosphorylation are used, it is possible that in some cells, the mimicking is not as efficient as in other cells. This is the limitation of using such mutants to investigate the contribution of phosphorylation in a cellular process. However, the results with these tau mutants do not rule out the possibility that phosphorylation sites other than the ones included in our mutants could modulate tau secretion by N2a cells.

In both physiological and pathological conditions, tau is released by neurons. The presence of extracellular tau in physiological conditions indicates that extracellular tau could have a beneficial role. This is the case of other cytosolic proteins such as annexins A4 and A5 acting as anticoagulants in the extracellular space (27). The role of tau in the extracellular space is still elusive. Dephosphorylated tau as detected in the medium was shown to be able to bind and activate muscarinic receptors (73, 74). However, it is still not clear if the concentration of tau in normal conditions could activate these receptors. In pathological conditions, extracellular pathological tau species are believed to be involved in the propagation of tau pathology in the brain and to affect the function of synapses by altering their protein composition (31, 75). In a recent study, the secretion factor of tau was evaluated to be between 10^{-5} and 10^{-6} depending on the brain region (76). In CSF, the tau concentration is 300 ng/liter in healthy individuals and 900 ng/liter in AD patients (68). The amount of tau released by neurons in culture is also very low (~20 ng/ml) (42). The low release of tau in the extracellular space could appear to be a secretory mechanism of tau species having an extracellular function rather than a tau clearance mechanism. However, this low amount of released tau does not exclude the possibility that secretion is a clearance mechanism. For example, released tau could correspond to the pool accumulating in the endolysosomal system and the secretion of this pool might be sufficient to prevent any tau-induced damages of this system as tau was shown to alter membrane integrity (77). Such a scenario was reported for α-synuclein that was shown to accumulate in mitochondria and to alter their function. Mitochondrial dysfunction could be rescued by increasing α-synuclein secretion (32).

We demonstrated that tau secretion can be increased by the overexpression of a SNARE associated with late endosomes. Most importantly, this was accompanied by a decrease of intracellular tau. It remains to be determined whether such an

overexpression could become a therapeutic strategy to prevent intracellular accumulation and aggregation of tau. Several studies have demonstrated that the reduction of intracellular tau can significantly slow down the progression of tau pathology resulting in improvement of functional deficits in tauopathy animal models (33). In the present study, we reported that tau secretion was efficient in reversing the stabilizing effects of tau on microtubules. Antisense oligonucleotides are currently being tested in clinical trials in mild AD patients (ClinicalTrials.gov identifier: NCT03186989). The intracellular accumulation of tau is believed to occur because tau degradation is less efficient. Drugs aiming at increasing tau degradation are presently under investigation (78). In such a context, increased tau secretion could be an alternative clearance mechanism to deficient tau degradation. However, all the strategies that are currently tested for reducing intracellular tau do not present specificity for affected neurons. Indeed, in AD, tau pathology begins in certain areas before spreading in the brain. The decrease of intracellular tau in regions nonaffected could have negative effects that could mask the beneficial effects resulting from a tau decrease in the affected regions. Consequences of tau reduction were reported in recent studies. Tau deletion was correlated to brain iron accumulation, brain insulin resistance, and alterations of synaptic plasticity and function and cognitive deficits (79–81). Our results indicate that overexpression of VAMP8 would be a suitable approach to decrease tau solely in regions affected by tau pathology because it did not increase the secretion of tau in control hippocampal slices but only when tau was overexpressed mimicking the accumulation of tau in affected neurons. The drawback of such an approach is the increase of extracellular pathological species that could favor the propagation of tau pathology in the brain and synaptic dysfunction. Our present results revealed that VAMP8 overexpression did not increase the formation of oligomeric tau and tau species presenting pathological conformational changes. From these data, one can conclude that VAMP8-induced secretion would not enhance the formation of tau toxic species if used as a therapeutic strategy to prevent intracellular tau accumulation. The presence of tau in the CSF in physiological conditions could indicate that certain tau species exert beneficial effects on neurons and therefore the increase of tau in the CSF at early stages of AD could be a neuroprotective response. In such a case, VAMP8 overexpression could be used to enhance the amount of released tau at early stages of AD to enhance tau-induced beneficial effects (68). During the progression of the disease, the increase of tau in the CSF is correlated with cognitive decline in patients (68, 76). This decline could correspond to the release of tau species altering synaptic function and therefore the increase of their release by VAMP8 overexpression could become detrimental to neurons. Because of this, it is imperative to identify tau species that are released upon VAMP8 overexpression and to determine their extracellular function. This will help to design antibodies that can solely sequester the toxic tau species without affecting the species that are beneficial to neurons.

The most efficient therapeutic approach for preventing intracellular tau accumulation remains to be developed. In the present study, we demonstrated that activating tau secretion by the late endosomal pathway could be a suitable approach that deserves to be further investigated. From the above observations, one can speculate that the increase of tau secretion to prevent tau intracellular accumulation combined with the capture of extracellular toxic tau by an antibody to abolish the propagation of tau pathology in the brain could be an efficient approach to prevent tau-induced neurodegeneration.

Materials and methods

Cell culture

N2a cells were purchased from ATCC (number CCL-131TM, Manassas, VA, USA) and were cultured in minimal essential medium with Earle's salt, nonessential amino acids supplemented with L-glutamine, sodium pyruvate, and sodium bicarbonate (Wisent Life Sciences, Saint Bruno, QC, Canada), and with 10% fetal bovine serum premium (Wisent Life Sciences) at 37 °C in a humidified 5% CO_2 incubator.

Culture of murine hippocampal slices and lentivirus transduction

Organotypic hippocampal slices were prepared and cultured from postnatal days 4–5 (P4–P5) C57BL/6 mice as described by Stoppini *et al.* (82). The mice were obtained from the colony of Dr. Catherine Larochelle at the CRCHUM. The use of animals and all experimental procedures described were carried out according to *The guide to the Care and Use of Experimental Animals of the Canadian Council on Animal Care.* The ethical approval was obtained from the Animal Care and Ethics Committee of the Centre de Recherche du Centre Hospitalier de l'Université de Montréal (CRCHUM) (protocol number N17012CLs). Briefly, mice were decapitated, brains were removed, and hippocampi were isolated and cut into 300-μm thick slices using a McIlwain tissue chopper. Slices were cultured using the membrane interface method on membrane culture inserts (0.4 μm, Millicell CM, EMD Millipore, Etobicoke, ON, Canada) in 6-well–plates containing 1 ml of culture medium (50% minimum essential medium, 25% basal medium Eagle's without glutamine, 25% heat-inactivated horse serum, 2 mM glutamine, 0.6% glucose, pH 7.2). Cultures were kept at 37 °C in a humidified atmosphere with 5% CO_2. Slices were kept in culture for 48 h allowing them to become adherent to the substrate filters before performing the experiments.

Lentivirus encoding either GFP, Tau, or VAMP8 was purchased from Applied Biological Materials Inc. (ABM, Richmond, BC, Canada). Slices were transduced by adding a suspension of lentivirus at a concentration of 3.8×10^7 PFU/ml directly on the slices and then a thin strip of filter membrane was applied to the slices. Twenty-four h after transduction, the membrane strip was removed. The culture medium was collected and replaced every 2 days.

Chemicals, antibodies, and plasmids

Chloroquine diphosphate salt (number C6628, Sigma, Oakville, ON, Canada) and MG-132 (number M8699, Sigma) were used at a final concentration of 100 μM for 4 h and 20 μM for 24 h, respectively. Bafilomycin A1 (number CM110-0100

Cedarlane®, Burlington, ON, Canada) was used at 25 nM for 20 h. For immunoblotting and dot blot, the following antibodies were used: total tau (1:50,000, number A0024, Dako, Santa Clara, CA, USA), GFP (1:1,000, number 3H9, Chromotek Inc., Hauppauge, NY, USA), ɣ-actin (1:10,000, number Sc-65635, Santa Cruz, Dallas, TX, USA), tau-1 (1:10,000, number MAB3420, EMD Millipore, Etobicoke, ON, Canada), tau-46 (1:500, number ab203179, Abcam, Cambridge, UK); AT180 (1:100, number MN1040, Thermo Fisher Scientific, Waltham, MA, USA), S199-202 (1:1,000, number 44-768G, Invitrogen, Carlsbad, CA, USA); c-myc (1:500, number M5546, Sigma); α-synuclein (1:1,000, number 610787, BD Transduction Laboratories, Franklin Lakes, NJ, USA), ubiquitin (1:500, number 3936, Cell Signaling Technology, Danvers, MA, USA), LC3 (1:1,000, number ab51520, Abcam), tau22 (1:10,000, number ABN454, EMD Millipore), and MC1 (1:500, gift from Peter Davies). For immunofluorescence microscopy, the antibody A0024 (1:1,000, Dako) was used. For the staining of the organotypic hippocampal slices, NeuN antibody (1:200, number N2173-20, U.S. Biological, Salem, MA, USA) and 4′,6-diamidino-2-phenylindole (1:1,000, number D9542-10MG, Sigma) were used. Plasmids FLAG-4R-TAU and pEGFP-C1 empty vector used for co-transfection of N2a cells were described previously (50). The plasmid GFP-VAMP8 was purchased from Addgene (number 42311, Cambridge, MA, USA). Flag-4R-TAU-P301L and Flag-4R-TAU-R406W were obtained by single site-directed mutagenesis from Flag-4R-TAU (Civic Biosciences limitée, Beloeil, QC, Canada). pEGFP-C1-A12 and pEGFP-C1-E12 were obtained by PCR-based mutagenesis from pEGFP-C1-4R-TAU to which the GFP tag was removed (Mutagenex, Suwanee, GA, USA) (50). Myc-α-Synuclein was obtained from Dr. E. A. Fon.

Western blotting

The culture medium of N2a cells containing tau was collected 48 h after transfection and centrifuged at 3000 rpm for 10 min at 23 °C to remove cell debris. The medium was mixed with Laemmli sample buffer once. For cell lysates, cells were washed twice with PBS and once with PBS containing 0.5 M NaCl and lysed in fresh lysis buffer containing Tris 50 mM, NaCl 300 mM, Triton X-100 (0.5%), a protease inhibitor mixture (Complete EDTA-free, Roche Diagnostics, Indianapolis, IN), and a phosphatase inhibitor mixture (PhosSTOP, Roche Diagnostics), and then incubated on ice for 20 min. Proteins were quantified using Bio-Rad DC Protein assay (Bio-Rad Laboratories Ltd., Mississauga, ON, Canada). The lysates were mixed with Laemmli buffer once and boiled for 5 min at 95 °C. Equal amounts of the culture medium and cell lysates were loaded in each lane and electrophoresed on polyacrylamide gels. Immunoblotting was performed as previously described (50). All the secondary antibodies used to reveal the primary antibodies were coupled with horseradish peroxidase and were purchased from Jackson ImmunoResearch (West Grove, PA, USA). For quantification of the immunoreactive bands, Western blotting image acquisition was performed using a Chemi-Doc MP system (Bio-Rad Laboratories, Hercules, CA, USA) and densitometry analysis was done with Image Laboratory software (version 5.0, Bio-Rad Laboratories).

Mesoscale immunoassay to measure total tau and tau phosphorylated at Thr-231

To measure total tau and tau phosphorylated at Thr-231, the lysate and the culture medium from N2a cells were prepared as described for Western blots. The amount of total tau and phosphorylated tau was determined by MSD MULTI-SPOT Phospho(Thr-231)/total Tau assay (number K15121D, Meso Scale Diagnostics, Rockville, MD, USA). This sensitive assay was used according to the manufacturer's instructions. A duplicate was used for each sample. All replicates were analyzed in a 96-well 4-spot plate at the same time. The plate was read with QuickPlex SQ120, a Meso Scale Diagnostics instrument.

The culture medium of organotypic hippocampal slices was collected and centrifuged at 3000 rpm for 10 min at room temperature to remove cell debris. The amount of total Tau in the medium was determined by MSD MULTI-SPOT mouse total Tau assay (number K151DSD, Meso Scale Diagnostics). The assay was used according to the manufacturer's instructions. A duplicate was used for each sample. All replicates were analyzed in a 96-well 4-spot plate at the same time. The plate was read with QuickPlex SQ120, a Meso Scale Diagnostics instrument.

Dot blot

The culture medium of N2a cells co-transfected either with Flag-4R-TAU and pEGFP-C1 empty vector or Flag-4R-TAU and GFP-VAMP8 was loaded (250 μl) on a nitrocellulose membrane 0.2 μm placed in the dot blot apparatus. The samples were filtered through passively for 1 h and then the vacuum flow was turned on to complete the filtration. Dot blot was revealed as described above for the Western blotting.

Immunofluorescence

N2a cells were grown on coverslips coated with poly-D-lysine (Mandel Scientific Co. Inc., Guelph, ON, Canada). The medium was changed 30 min before fixation to stimulate Tau secretion. Then, the cells were fixed in 4% PFA/PBS for 10 min at 37 °C and permeabilized with 0.2% Triton X-100 in PBS for 5 min. All the solutions for the immunofluorescence were prepared in PBS (×1). Coverslips were blocked with 5% normal goat serum (Invitrogen) in PBS. Then coverslips were stained with the primary antibody, A0024 diluted in PBS (1:1000, Dako) at room temperature for 1 h. After 3 washes in PBS, coverslips were incubated with the secondary antibody coupled to FITC (Jackson ImmunoResearch) at room temperature for 1 h. Coverslips were then washed in PBS and mounted in Mowiol. Labeled cells were visualized with an Apotome Axio Imager M2 Zeiss microscope using ×63 objective.

The organotypic hippocampal slices were fixed in 4% PFA in PBS for 3 × 20 min at room temperature. After one wash in PBS for 10 min and one wash in 0.05% PBST for 10 min, the slices were blocked with the Endogeneous Biotin Blocking kit (number E21390, Invitrogen) according to the manufacturer's instructions. Slices were stained with NeuN antibody diluted in

0.05% PBST at 4 °C overnight. After 5 washes in PBS, slices were incubated with streptavidine A674 (number S32357, Invitrogen) at room temperature for 3 h. After 2 washes in PBS, slices were stained with 4′,6-diamidino-2-phenylindole (1:1000). They were then washed in PBS and mounted in ProLong Gold antifade reagent (number P36934, Invitrogen). Slices were visualized with SP5 Leica microscope using ×63 objective.

TIRF microscopy

N2a cells grown on an 35-mm imaging dish with a glass bottom (number 81158, Ibidi, Gräfelfing, Bayern, Germany) were transfected for 48 h with tau and VAMP8 plasmids. Thirty minutes before imaging, the medium was changed to stimulate tau secretion. TIRF images were acquired using a Zeiss Axio Observer Z.1 inverted microscope (Zeiss, Oberkochen, Germany) coupled with a TIRF fiber unit. Cells were maintained under a 37 °C, 5% CO_2 and humidity environment using a TokaiHit top stage chamber (TokaiHit, Japan). All images were acquired using a αPlan-Apochromat ×100/1.46 NA (numerical aperture) OIL objective and an AxioCam MR R3 camera (1036 × 1040) giving a 65-nm pixel resolution. For excitation, 561 (50 mW) and 488 nm (20 mW) diode pump solid state lasers (Coherent, Santa Clara, CA, USA) were used for RFP and GFP, respectively. Live images were acquired as follows: 1) TIRF angle was set on a representative cell; 2) definite focus module was used to stabilize the focus over time (activated every 20 time points); 3) a quadruple filter set (77HE: 506/582/659) was used for fast detection; 4) GFP and RFP signals were acquired sequentially with a 20-ms exposure time for each; and 5) the images were acquired every 517 ms (±10 ms) for 2 min. Images were acquired and analyzed using the Zen Blue software (Zeiss, Germany). Final images are 12 bits.

RNA extraction and qRT-PCR

Extraction of RNA from N2a cells was performed using an RNeasy Plus Mini Kit (Qiagen, Toronto, ON, Canada), following the manufacturer's instructions. Reverse transcription and real-time reaction were performed by the Genomics Core Facility of IRIC (Montréal, Québec, Canada). The measurement of TAU DNA content by real-time qPCR was performed using on a QuantStudio™ 7 flex system instrument, TaqMan® Reagents and analyzed with QuantStudio Real-Time PCR software (Applied Biosystems, Foster, CA, USA). Two endogenous controls were used, ACTB and GAPDH. Calculation of relative quantifications values is described in Livak *et al.* (83) according to the $2^{-\Delta\Delta CT}$ method (RQ).

Calculation of normalized tau secretion

In all the graphs presenting the quantification of tau secretion by Western blotting, normalized tau secretion was calculated. To calculate normalized tau secretion, the signal of total tau in the medium (ExTau) was divided by the signal of total tau in the cell lysate (InTau). The signal of InTau was normalized to that of actin in the cell lysate.

LDH assay

LDH activity in media was determined using a LDH Activity Assay Kit (Cayman Chemical Company, Ann Arbor, MI, USA) according to manufacturer's instructions. The LDH content in the samples was measured using a BIO-TEK SYNERGY4 plate reader at $A_{490\ nm}$ (Winooski, VT, USA). The mean of the enzyme activity was used for comparison between experimental conditions.

Quantification of the co-localization of VAMP8 and Rabs

N2a cells transfected either with Flag-tau/RFP-VAMP8/GFP-Rab7, Flag-tau/RFP-VAMP8/GFP-Rab9, or Flag-tau/RFP-VAMP8/GFP-Rab11 were grown on coverslips coated with poly-D-lysine (Mandel Scientific). After 48 h transfection, the cells were fixed in 4% PFA/PBS for 10 min at 37 °C. Coverslips were then washed in PBS and mounted in Mowiol. Transfected cells were visualized with an Apotome Axio Imager M2 Zeiss microscope using ×63 objective.

The co-localization was quantified with Imaris Software (version 9.3.1 Biplane, Belfast, United Kingdom) with the coloc module. The quantification was represented by Pearson's coefficient.

Statistical analysis

The statistical analysis was performed using Prism 8.0c software (GraphPad Software Inc., San Diego, CA, USA). Findings were considered significant as follows: *, $p < 0.05$; **, $p < 0.01$; ***$p < 0.001$, or ****, $p < 0.0001$. For all the experiments, statistical significance was evaluated with paired *t* test unless otherwise stated. For tau secretion by hippocampal slices, we baselined each value with its control and for statistical significance, a paired analysis of variance test followed by a pairwise *t* test was used. The *p* values were adjusted with the Bonferroni correction. To verify the reproducibility of the co-localization of VAMP8 with a Rab from three independent experiments, a χ square was performed. Statistical significance for the quantification of VAMP8 co-localization with a Rab was evaluated with a Mann Whitney two-tailed unpaired *t* test.

Data availability

All data are contained within this article and the supporting information.

Acknowledgments—We thank the Genomics core facility of IRIC (Montréal, Québec, Canada) for the qPCR analysis. We also thank Aurélie Cleret-Buhot of the Cell Imaging core facility of the CRCHUM (Montréal, Québec, Canada) for performing the TIRF microscopy acquisitions and Maude Gelinas-Faucher for her help with the Western blot analysis. We are grateful to Olivier Tastet and Ali Filali for their help with the statistical analysis. We also thank Dr. Thierry Galli for the construct GFP-VAMP8 obtained from Addgene. Last, we thank all the laboratory members for helpful discussions.

Author contributions—J. P., A. D., E. A. F., and N. L. conceptualization; J. P., A. D., C. P., and H. J. formal analysis; J. P., A. D., C. P.,

and H. J. methodology; J. P. project administration; J. P., C. P., H. J., C. L., E. A. F., and N. L. writing-review and editing; C. L. resources; C. L. and N. L. supervision; E. A. F. and N. L. funding acquisition; N. L. writing-original draft.

Funding and additional information—This work was supported in part by Canadian Institute of Health Research (CIHR) Grant PJT-155993 (to N. L. and E. A. F.) and from CRCHUM internal funds (to N. L.).

Conflict of interest—The authors declare that they have no conflicts of interest with the contents of this article.

Abbreviations—The abbreviations used are: AD, Alzheimer disease; FTDP, frontotemporal dementia with parkinsonism; FTLD, frontotemporal lobe degeneration; CSF, cerebrospinal fluid; VAMP-8, vesicle-associated membrane protein 8; SNARE, soluble NSF attachment protein receptor; LDH, lactase dehydrogenase; TIRF, total internal reflection fluorescence; qPCR, quantitative PCR; PFA, paraformaldehyde; GAPDH, glyceraldehyde-3-phosphate dehydrogenase; MAP, microtubule-associated protein.

References

1. Ludin, B., and Matus, A. (1993) The neuronal cytoskeleton and its role in axonal and dendritic plasticity. *Hippocampus* **3 Spec No,** 61–71 CrossRef Medline
2. Mandell, J., and Banker, G. (1996) Microtubule-associated proteins, phosphorylation gradients, and the establishment of neuronal polarity. *Perspect. Dev. Neurobiol.* **4,** 125– 135 Medline
3. Iqbal, K., Liu, F., and Gong, C. X. (2016) Tau and neurodegenerative disease: the story so far. *Nat. Rev. Neurol.* **12,** 15–27 CrossRef Medline
4. Lee, V., Goedert, M., and Trojanowski, J. (2001) Neurodegenerative tauopathies. *Annu. Rev. Neurosci* **24,** 1121– 1159 CrossRef Medline
5. Cairns, N. J., Bigio, E. H., Mackenzie, I. R., Neumann, M., Lee, V. M., Hatanpaa, K. J., White, C. L., 3rd, Schneider, J. A., Grinberg, L. T., Halliday, G., Duyckaerts, C., Lowe, J. S., Holm, I. E., Tolnay, M., Okamoto, K., *et al.* Consortium for Frontotemporal Lobar Degeneration (2007) Neuropathologic diagnostic and nosologic criteria for frontotemporal lobar degeneration: consensus of the Consortium for Frontotemporal Lobar Degeneration. *Acta Neuropathol.* **114,** 5–22 CrossRef Medline
6. Alafuzoff, I., Iqbal, K., Friden, H., Adolfsson, R., and Winblad, B. (1987) Histopathological criteria for progressive dementia disorders: clinical-pathological correlation and classification by multivariate data analysis. *Acta Neuropathol.* **74,** 209–225 CrossRef Medline
7. Arriagada, P., Growdon, J., Hedley-Whyte, E., and Hyman, B. (1992) Neurofibrillary tangles but not senile plaques parallel duration and severity of Alzheimer's disease. *Neurology* **42,** 631–639 CrossRef Medline
8. Bierer, L., Hof, P., Purohit, D., Carlin, L., Schmeidler, J., Davis, K., and Perl, D. (1995) Neocortical neurofibrillary tangles correlate with dementia severity in Alzheimer's disease. *Arch. Neurol.* **52,** 81–88 CrossRef Medline
9. Braak, H., and Braak, E. (1991) Neuropathological staging of Alzheimer-related changes. *Acta Neuropathol.* **82,** 239–259 CrossRef Medline
10. Tomlinson, B. E., Blessed, G., and Roth, M. (1970) Observations on the brains of demented old people. *J. Neurol. Sci.* **11,** 205–242 CrossRef Medline
11. Ossenkoppele, R., Schonhaut, D. R., Schöll, M., Lockhart, S. N., Ayakta, N., Baker, S. L., O'Neil, J. P., Janabi, M., Lazaris, A., Cantwell, A., Vogel, J., Santos, M., Miller, Z. A., Bettcher, B. M., Vossel, K. A., *et al.* (2016) Tau PET patterns mirror clinical and neuroanatomical variability in Alzheimer's disease. *Brain* **139,** 1551–1567 CrossRef
12. Pontecorvo, M. J., Devous, M. D., Kennedy, I., Navitsky, M., Lu, M., Galante, N., Salloway, S., Doraiswamy, P. M., Southekal, S., Arora, A. K., McGeehan, A., Lim, N. C., Xiong, H., Truocchio, S. P., Joshi, A. D., *et al.* (2019) A multicentre longitudinal study of flortaucipir (18F) in normal ageing, mild cognitive impairment and Alzheimer's disease dementia. *Brain* **142,** 1723–1735 CrossRef Medline
13. Hutton, M., Lendon, C. L., Rizzu, P., Baker, M., Froelich, S., Houlden, H., Pickering-Brown, S., Chakraverty, S., Isaacs, A., Grover, A., Hackett, J., Adamson, J., Lincoln, S., Dickson, D., Davies, P., *et al.* (1998) Association of missense and 5'-splice-site mutations in tau with the inherited dementia FTDP-17. *Nature* **393,** 702–705 CrossRef Medline
14. Poorkaj, P., Bird, T. D., Wijsman, E., Nemens, E., Garruto, R. M., Anderson, L., Andreadis, A., Wiederholt, W. C., Raskind, M., and Schellenberg, G. D. (1998) Tau is a candidate gene for chromosome 17 frontotemporal dementia. *Ann. Neurol.* **43,** 815–825 CrossRef Medline
15. Kumar-Singh, S., and Van Broeckhoven, C. (2007) Frontotemporal lobar degeneration: current concepts in the light of recent advances. *Brain Pathol.* **17,** 104–114 CrossRef Medline
16. Poorkaj, P., Grossman, M., Steinbart, E., Payami, H., Sadovnick, A., Nochlin, D., Tabira, T., Trojanowski, J. Q., Borson, S., Galasko, D., Reich, S., Quinn, B., Schellenberg, G., and Bird, T. D. (2001) Frequency of tau gene mutations in familial and sporadic cases of non-Alzheimer dementia. *Arch Neurol.* **58,** 383–387 CrossRef Medline
17. Rademakers, R., Cruts, M., and van Broeckhoven, C. (2004) The role of tau (MAPT) in frontotemporal dementia and related tauopathies. *Hum. Mutat.* **24,** 277–295 CrossRef Medline
18. Ghetti, B., Oblak, A. L., Boeve, B. F., Johnson, K. A., Dickerson, B. C., and Goedert, M. (2015) Invited review: Frontotemporal dementia caused by microtubule-associated protein tau gene (MAPT) mutations: a chameleon for neuropathology and neuroimaging. *Neuropathol. Appl. Neurobiol.* **41,** 24–46 CrossRef Medline
19. Schraen-Maschke, S., Dhaenens, C. M., Delacourte, A., and Sablonnière, B. (2004) Microtubule-associated protein tau gene: a risk factor in human neurodegenerative diseases. *Neurobiol. Dis.* **15,** 449–460 CrossRef Medline
20. Le Guennec, K., Quenez, O., Nicolas, G., Wallon, D., Rousseau, S., Richard, A. C., Alexander, J., Paschou, P., Charbonnier, C., Bellenguez, C., Grenier-Boley, B., Lechner, D., Bihoreau, M. T., Olaso, R., Boland, A., *et al.* (2017) 17q21.31 duplication causes prominent tau-related dementia with increased MAPT expression. *Mol. Psychiatry* **22,** 1119–1125 CrossRef Medline
21. Hampel, H., Blennow, K., Shaw, L. M., Hoessler, Y. C., Zetterberg, H., and Trojanowski, J. Q. (2010) Total and phosphorylated tau protein as biological markers of Alzheimer's disease. *Exp. Gerontol.* **45,** 30–40 CrossRef Medline
22. Yamada, K., Cirrito, J. R., Stewart, F. R., Jiang, H., Finn, M. B., Holmes, B. B., Binder, L. I., Mandelkow, E. M., Diamond, M. I., Lee, V. M., and Holtzman, D. M. (2011) *In vivo* microdialysis reveals age-dependent decrease of brain interstitial fluid tau levels in P301S human tau transgenic mice. *J. Neurosci.* **31,** 13110–13117 CrossRef Medline
23. Pooler, A. M., Phillips, E. C., Lau, D. H., Noble, W., and Hanger, D. P. (2013) Physiological release of endogenous tau is stimulated by neuronal activity. *EMBO Rep.* **14,** 389–394 CrossRef Medline
24. Yamada, K., Holth, J. K., Liao, F., Stewart, F. R., Mahan, T. E., Jiang, H., Cirrito, J. R., Patel, T. K., Hochgräfe, K., Mandelkow, E. M., and Holtzman, D. M. (2014) Neuronal activity regulates extracellular tau *in vivo*. *J. Exp. Med.* **211,** 387–393 CrossRef Medline
25. Mohamed, N. V., Plouffe, V., Rémillard-Labrosse, G., Planel, E., and Leclerc, N. (2014) Starvation and inhibition of lysosomal function increased tau secretion by primary cortical neurons. *Sci. Rep.* **4,** 5715 CrossRef Medline
26. Barthélemy, N. R., Gabelle, A., Hirtz, C., Fenaille, F., Sergeant, N., Schraen-Maschke, S., Vialaret, J., Buee, L., Junot, C., Becher, F., and Lehmann, S. (2016) Differential mass spectrometry profiles of tau protein in the cerebrospinal fluid of patients with Alzheimer's disease, progressive supranuclear palsy, and dementia with Lewy bodies. *J. Alzheimers Dis.* **51,** 1033–1043 CrossRef Medline
27. Gerke, V., and Moss, S. E. (2002) Annexins: from structure to function. *Physiol. Rev.* **82,** 331–371 CrossRef Medline
28. Iguchi, Y., Eid, L., Parent, M., Soucy, G., Bareil, C., Riku, Y., Kawai, K., Takagi, S., Yoshida, M., Katsuno, M., Sobue, G., and Julien, J. P. (2016)

Exosome secretion is a key pathway for clearance of pathological TDP-43. *Brain* **139,** 3187–3201 CrossRef Medline
29. Mohamed, N. V., Herrou, T., Plouffe, V., Piperno, N., and Leclerc, N. (2013) Spreading of tau pathology in Alzheimer's disease by cell-to-cell transmission. *Eur. J. Neurosci.* **37,** 1939–1948 CrossRef Medline
30. Goedert, M., and Spillantini, M. G. (2017) Propagation of Tau aggregates. *Mol. Brain* **10,** 18 CrossRef Medline
31. Pernegre, C., Duquette, A., and Leclerc, N. (2019) Tau secretion: good and bad for neurons. *Front. Neurosci.* **13,** 649 CrossRef Medline
32. Tsunemi, T., Perez-Rosello, T., Ishiguro, Y., Yoroisaka, A., Jeon, S., Hamada, K., Rammonhan, M., Wong, Y. C., Xie, Z., Akamatsu, W., Mazzulli, J. R., Surmeier, D. J., Hattori, N., and Krainc, D. (2019) Increased lysosomal exocytosis induced by lysosomal Ca^{2+} channel agonists protects human dopaminergic neurons from α-synuclein toxicity. *J. Neurosci.* **39,** 5760–5772 CrossRef Medline
33. Jadhav, S., Avila, J., Schöll, M., Kovacs, G. G., Kovari, E., Skrabana, R., Evans, L. D., Kontsekova, E., Malawska, B., de Silva, R., Buee, L., and Zilka, N. (2019) A walk through tau therapeutic strategies. *Acta Neuropathol. Commun.* **7,** 22 CrossRef Medline
34. Rodriguez, L., Mohamed, N.-V., Desjardins, A., Lippé, R., Fon, E. A., and Leclerc, N. (2017) Rab7A regulates tau secretion. *J. Neurochem.* **141,** 592–605 CrossRef Medline
35. Antonin, W., Holroyd, C., Tikkanen, R., Höning, S., and Jahn, R. (2000) The R-SNARE endobrevin/VAMP-8 mediates homotypic fusion of early endosomes and late endosomes. *Mol. Biol. Cell* **11,** 3289–3298 CrossRef Medline
36. Itakura, E., Kishi-Itakura, C., and Mizushima, N. (2012) The hairpin-type tail-anchored SNARE syntaxin 17 targets to autophagosomes for fusion with endosomes/lysosomes. *Cell* **151,** 1256–1269 CrossRef Medline
37. Pryor, P. R., Mullock, B. M., Bright, N. A., Lindsay, M. R., Gray, S. R., Richardson, S. C., Stewart, A., James, D. E., Piper, R. C., and Luzio, J. P. (2004) Combinatorial SNARE complexes with VAMP7 or VAMP8 define different late endocytic fusion events. *EMBO Rep.* **5,** 590–595 CrossRef Medline
38. Wang, C. C., Ng, C. P., Lu, L., Atlashkin, V., Zhang, W., Seet, L. F., and Hong, W. (2004) A role of VAMP8/endobrevin in regulated exocytosis of pancreatic acinar cells. *Dev. Cell* **7,** 359–371 CrossRef Medline
39. Wang, C. C., Shi, H., Guo, K., Ng, C. P., Li, J., Gan, B. Q., Chien Liew, H., Leinonen, J., Rajaniemi, H., Zhou, Z. H., Zeng, Q., and Hong, W. (2007) VAMP8/endobrevin as a general vesicular SNARE for regulated exocytosis of the exocrine system. *Mol. Biol. Cell* **18,** 1056–1063 CrossRef Medline
40. Marshall, M. R., Pattu, V., Halimani, M., Maier-Peuschel, M., Müller, M. L., Becherer, U., Hong, W., Hoth, M., Tschernig, T., Bryceson, Y. T., and Rettig, J. (2015) VAMP8-dependent fusion of recycling endosomes with the plasma membrane facilitates T lymphocyte cytotoxicity. *J. Cell Biol.* **210,** 135–151 CrossRef Medline
41. Zhu, D., Zhang, Y., Lam, P. P., Dolai, S., Liu, Y., Cai, E. P., Choi, D., Schroer, S. A., Kang, Y., Allister, E. M., Qin, T., Wheeler, M. B., Wang, C. C., Hong, W. J., Woo, M., *et al.* (2012) Dual role of VAMP8 in regulating insulin exocytosis and islet beta cell growth. *Cell Metab.* **16,** 238–249 CrossRef Medline
42. Mohamed, N.-V., Desjardins, A., and Leclerc, N. (2017) Tau secretion is correlated to an increase of Golgi dynamics. *PLoS ONE* **12,** e0178288 CrossRef Medline
43. Tang, M., Harrison, J., Deaton, C. A., and Johnson, G. V. W. (2019) Tau clearance mechanisms. *Adv. Exp. Med. Biol.* **1184,** 57–68 CrossRef Medline
44. Cho, J. H., and Johnson, G. V. (2004) Primed phosphorylation of tau at Thr231 by glycogen synthase kinase 3β (GSK3β) plays a critical role in regulating tau's ability to bind and stabilize microtubules. *J. Neurochem.* **88,** 349–358 CrossRef Medline
45. Takemura, R., Okabe, S., Umeyama, T., Kanai, Y., Cowan, N. J., and Hirokawa, N. (1992) Increased microtubule stability and α tubulin acetylation in cells transfected with microtubule-associated proteins MAP1B, MAP2 or tau. *J. Cell Sci.* **103,** 953–964 Medline
46. Bright, J., Hussain, S., Dang, V., Wright, S., Cooper, B., Byun, T., Ramos, C., Singh, A., Parry, G., Stagliano, N., and Griswold-Prenner, I. (2015) Human secreted tau increases amyloid-beta production. *Neurobiol. Aging* **36,** 693–709 CrossRef Medline
47. Wandinger-Ness, A., and Zerial, M. (2014) Rab proteins and the compartmentalization of the endosomal system. *Cold Spring Harbor Perspect. Biol.* **6,** a022616 CrossRef Medline
48. Feng, Y., Press, B., and Wandinger-Ness, A. (1995) Rab 7: an important regulator of late endocytic membrane traffic. *J. Cell Biol.* **131,** 1435–1452 CrossRef Medline
49. Kucera, A., Bakke, O., and Progida, C. (2016) The multiple roles of Rab9 in the endolysosomal system. *Commun. Integr. Biol.* **9,** e1204498 CrossRef Medline
50. Plouffe, V., Mohamed, N. V., Rivest-McGraw, J., Bertrand, J., Lauzon, M., and Leclerc, N. (2012) Hyperphosphorylation and cleavage at D421 enhance tau secretion. *PLoS ONE* **7,** e36873 CrossRef Medline
51. Dujardin, S., Begard, S., Caillierez, R., Lachaud, C., Delattre, L., Carrier, S., Loyens, A., Galas, M. C., Bousset, L., Melki, R., Aurégan, G., Hantraye, P., Brouillet, E., Buee, L., and Colin, M. (2014) Ectosomes: a new mechanism for non-exosomal secretion of tau protein. *PLoS ONE* **9,** e100760 CrossRef Medline
52. Wang, Y., Balaji, V., Kaniyappan, S., Kruger, L., Irsen, S., Tepper, K., Chandupatla, R., Maetzler, W., Schneider, A., Mandelkow, E., and Mandelkow, E. M. (2017) The release and trans-synaptic transmission of Tau via exosomes. *Mol. Neurodegener.* **12,** 5 CrossRef Medline
53. Carmel, G., Mager, E. M., Binder, L. I., and Kuret, J. (1996) The structural basis of monoclonal antibody Alz50's selectivity for Alzheimer's disease pathology. *J. Biol. Chem.* **271,** 32789–32795 CrossRef Medline
54. Szendrei, G. I., Lee, V. M., and Otvos, L., Jr. (1993) Recognition of the minimal epitope of monoclonal antibody Tau-1 depends upon the presence of a phosphate group but not its location. *J. Neurosci. Res.* **34,** 243–249 CrossRef Medline
55. Lasagna-Reeves, C. A., Castillo-Carranza, D. L., Sengupta, U., Sarmiento, J., Troncoso, J., Jackson, G. R., and Kayed, R. (2012) Identification of oligomers at early stages of tau aggregation in Alzheimer's disease. *FASEB J.* **26,** 1946–1959 CrossRef Medline
56. Jicha, G. A., Bowser, R., Kazam, I. G., and Davies, P. (1997) Alz-50 and MC-1, a new monoclonal antibody raised to paired helical filaments, recognize conformational epitopes on recombinant tau. *J. Neurosci. Res.* **48,** 128–132 CrossRef Medline
57. Forrest, S. L., Kril, J. J., Stevens, C. H., Kwok, J. B., Hallupp, M., Kim, W. S., Huang, Y., McGinley, C. V., Werka, H., Kiernan, M. C., Götz, J., Spillantini, M. G., Hodges, J. R., Ittner, L. M., and Halliday, G. M. (2018) Retiring the term FTDP-17 as MAPT mutations are genetic forms of sporadic frontotemporal tauopathies. *Brain* **141,** 521–534 CrossRef Medline
58. Emmanouilidou, E., and Vekrellis, K. (2016) Exocytosis and spreading of normal and aberrant α-synuclein. *Brain Pathol.* **26,** 398–403 CrossRef Medline
59. Benskey, M. J., Perez, R. G., and Manfredsson, F. P. (2016) The contribution of α-synuclein to neuronal survival and function: Implications for Parkinson's disease. *J. Neurochem.* 137, 331–359 CrossRef Medline
60. Diaz-Vera, J., Palmer, S., Hernandez-Fernaud, J. R., Dornier, E., Mitchell, L. E., Macpherson, I., Edwards, J., Zanivan, S., and Norman, J. C. (2017) A proteomic approach to identify endosomal cargoes controlling cancer invasiveness. *J. Cell Sci.* **130,** 697–711 CrossRef Medline
61. Lee, J. G., Takahama, S., Zhang, G., Tomarev, S. I., and Ye, Y. (2016) Unconventional secretion of misfolded proteins promotes adaptation to proteasome dysfunction in mammalian cells. *Nat. Cell Biol.* **18,** 765–776 CrossRef Medline
62. Nixon, R. A. (2005) Endosome function and dysfunction in Alzheimer's disease and other neurodegenerative diseases. *Neurobiol. Aging* **26,** 373–382 CrossRef Medline
63. Ginsberg, S. D., Alldred, M. J., Counts, S. E., Cataldo, A. M., Neve, R. L., Jiang, Y., Wuu, J., Chao, M. V., Mufson, E. J., Nixon, R. A., and Che, S. (2010) Microarray analysis of hippocampal CA1 neurons implicates early endosomal dysfunction during Alzheimer's disease progression. *Biol. Psychiatry* **68,** 885–893 CrossRef Medline
64. Ginsberg, S. D., Mufson, E. J., Alldred, M. J., Counts, S. E., Wuu, J., Nixon, R. A., and Che, S. (2011) Upregulation of select rab GTPases in cholinergic

basal forebrain neurons in mild cognitive impairment and Alzheimer's disease. *J. Chem. Neuroanat.* **42,** 102–110 CrossRef Medline
65. Ginsberg, S. D., Mufson, E. J., Counts, S. E., Wuu, J., Alldred, M. J., Nixon, R. A., and Che, S. (2010) Regional selectivity of rab5 and rab7 protein upregulation in mild cognitive impairment and Alzheimer's disease. *J. Alzheimers Dis.* **22,** 631–639 CrossRef Medline
66. Tiernan, C. T., Ginsberg, S. D., Guillozet-Bongaarts, A. L., Ward, S. M., He, B., Kanaan, N. M., Mufson, E. J., Binder, L. I., and Counts, S. E. (2016) Protein homeostasis gene dysregulation in pretangle-bearing nucleus basalis neurons during the progression of Alzheimer's disease. *Neurobiol. Aging* **42,** 80–90 CrossRef Medline
67. Russell, C. L., Mitra, V., Hansson, K., Blennow, K., Gobom, J., Zetterberg, H., Hiltunen, M., Ward, M., and Pike, I. (2017) Comprehensive quantitative profiling of tau and phosphorylated tau peptides in cerebrospinal fluid by mass spectrometry provides new biomarker candidates. *J. Alzheimers Dis.* **55,** 303–313 CrossRef Medline
68. Blennow, K., and Hampel, H. (2003) CSF markers for incipient Alzheimer's disease. *Lancet Neurol.* **2,** 605–613 CrossRef Medline
69. Wang, T., Zhang, M., Ma, Z., Guo, K., Tergaonkar, V., Zeng, Q., and Hong, W. (2012) A role of Rab7 in stabilizing EGFR-Her2 and in sustaining Akt survival signal. *J. Cell. Physiol.* **227,** 2788–2797 CrossRef Medline
70. Xu, Y., Cui, L., Dibello, A., Wang, L., Lee, J., Saidi, L., Lee, J. G., and Ye, Y. (2018) DNAJC5 facilitates USP19-dependent unconventional secretion of misfolded cytosolic proteins. *Cell Discov.* **4,** 11 CrossRef Medline
71. Vaz-Silva, J., Gomes, P., Jin, Q., Zhu, M., Zhuravleva, V., Quintremil, S., Meira, T., Silva, J., Dioli, C., Soares-Cunha, C., Daskalakis, N. P., Sousa, N., Sotiropoulos, I., and Waites, C. L. (2018) Endolysosomal degradation of Tau and its role in glucocorticoid-driven hippocampal malfunction. *EMBO J.* **37,** CrossRef
72. Gao, S., Casey, A. E., Sargeant, T. J., and Mäkinen, V. P. (2018) Genetic variation within endolysosomal system is associated with late-onset Alzheimer's disease. *Brain* **141,** 2711–2720 CrossRef Medline
73. Gómez-Ramos, A., Díaz-Hernández, M., Rubio, A., Miras-Portugal, M. T., and Avila, J. (2008) Extracellular tau promotes intracellular calcium increase through M1 and M3 muscarinic receptors in neuronal cells. *Mol. Cell. Neurosci.* **37,** 673–681 CrossRef Medline
74. Gómez-Ramos, A., Díaz-Hernández, M., Rubio, A., Díaz-Hernández, J. I., Miras-Portugal, M. T., and Avila, J. (2009) Characteristics and consequences of muscarinic receptor activation by tau protein. *Eur. Neuropsychopharmacol.* **19,** 708–717 CrossRef Medline
75. Shrivastava, A. N., Redeker, V., Pieri, L., Bousset, L., Renner, M., Madiona, K., Mailhes-Hamon, C., Coens, A., Buée, L., Hantraye, P., Triller, A., and Melki, R. (2019) Clustering of Tau fibrils impairs the synaptic composition of α3-Na^+/K^+-ATPase and AMPA receptors. *EMBO J.* **38,** CrossRef
76. Han, P., Serrano, G., Beach, T. G., Caselli, R. J., Yin, J., Zhuang, N., and Shi, J. (2017) A quantitative analysis of brain soluble tau and the tau secretion factor. *J. Neuropathol. Exp. Neurol.* **76,** 44–51 CrossRef Medline
77. Flach, K., Hilbrich, I., Schiffmann, A., Gärtner, U., Krüger, M., Leonhardt, M., Waschipky, H., Wick, L., Arendt, T., and Holzer, M. (2012) Tau oligomers impair artificial membrane integrity and cellular viability. *J. Biol. Chem.* **287,** 43223–43233 CrossRef Medline
78. Congdon, E. E., and Sigurdsson, E. M. (2018) Tau-targeting therapies for Alzheimer disease. *Nat. Rev. Neurol.* **14,** 399–415 CrossRef Medline
79. Ahmed, T., Van der Jeugd, A., Blum, D., Galas, M. C., D'Hooge, R., Buee, L., and Balschun, D. (2014) Cognition and hippocampal synaptic plasticity in mice with a homozygous tau deletion. *Neurobiol. Aging* **35,** 2474–2478 CrossRef Medline
80. Lei, P., Ayton, S., Finkelstein, D. I., Spoerri, L., Ciccotosto, G. D., Wright, D. K., Wong, B. X., Adlard, P. A., Cherny, R. A., Lam, L. Q., Roberts, B. R., Volitakis, I., Egan, G. F., McLean, C. A., Cappai, R., *et al.* (2012) Tau deficiency induces parkinsonism with dementia by impairing APP-mediated iron export. *Nat. Med.* **18,** 291–295 CrossRef Medline
81. Marciniak, E., Leboucher, A., Caron, E., Ahmed, T., Tailleux, A., Dumont, J., Issad, T., Gerhardt, E., Pagesy, P., Vileno, M., Bournonville, C., Hamdane, M., Bantubungi, K., Lancel, S., Demeyer, D., *et al.* (2017) Tau deletion promotes brain insulin resistance. *J. Exp. Med.* **214,** 2257–2269 CrossRef Medline
82. Stoppini, L., Buchs, P. A., and Muller, D. (1991) A simple method for organotypic cultures of nervous tissue. *J. Neurosci. Methods* **37,** 173–182 CrossRef Medline
83. Livak, K. J., and Schmittgen, T. D. (2001) Analysis of relative gene expression data using real-time quantitative PCR and the 2(-$\Delta\Delta C_T$) method. *Methods* **25,** 402–408 CrossRef Medline